Kobe University Repository : Kernel

PDF issue: 2025-12-05

Evaluation of speed loss in bulk carriers with actual data from rough sea voyages

Sasa, Kenji ; Takeuchi, Kaichi ; Chen, Chen ; Faltinsen, Odd Magnus ; Prpic-Orsic, Jasna ; Valcic, Marko ; Mrakovcic, Tomislav ; Herai, Naoki

(Citation)
Ocean Engineering,187:106162

(Issue Date)
2019-09-01

(Resource Type)
journal article

(Version)
Accepted Manuscript

(Rights)
© 2019 Elsevier Ltd.
This manuscript version is made available under the CC-BY-NC-ND 4.0 license
http://creativecommons.org/licenses/by-nc-nd/4.0/

(URL)
https://hdl.handle.net/20.500.14094/90007402

KOBE UNIVERSITY

Evaluation of Speed Loss in Bulk Carriers with Actual Data from Rough Sea Voyages

Kenji Sasa[*1], Kaichi Takeuchi[**], Chen Chen[*], Odd Magnus Faltinsen[***], Jasna Prpić-Oršić[****], Marko Valčić[****], Tomislav Mrakovčić[****], and Naoki Herai[*****]

* Department of Maritime Sciences, Kobe University, Kobe, Japan
5-1-1, Fukae Minami Machi, Higashinada-Ku, Kobe, 658-0022 Japan
E-mail: sasa@maritime.kobe-u.ac.jp (Corresponding Author: Kenji Sasa)
** Hitachi Zosen Corporation, Osaka, Japan
*** Centre for Autonomous Marine Operations and Systems, Norwegian University of Science and Technology, Trondheim, Norway
**** Faculty of Engineering, University of Rijeka, Rijeka, Croatia
***** Imabari Shipbuilding Co. Ltd., Marugame, Japan

Abstract

The evaluation of speed loss is the most important studies in the optimal ship routing. However, the mode of speed loss during rough sea voyages is complicated because of the involvement of the human factor. A speed loss analysis is conducted to improve the accuracy of evaluation of measured data extracted from actual marine conditions. First, the conventional criteria to judge the deliberate speed reduction is summarized with the conventional ship maneuvering techniques. Second, a nationwide questionnaire for marine engineers implemented for engine safety during rough sea voyages is detailed. Third, these conventional criteria are validated by analyzing the collated data on accelerations, ship motions, navigation, and engine parameters. The limiting value of vertical acceleration agrees with that obtained via practical measurements. On the contrary, the limiting values of lateral acceleration, roll motions, probabilities of deck wetness, and slamming do not agree with that obtained via measurements. The probabilities of deck wetness, slamming, and propeller racing start to increase at approximately the same instant where the deliberate speed reduction occurs. Some relations between the deck and engine parameters detailed in this paper were found to be highly correlated. Finally, the results of the analysis were used to model simpler estimations.

1. Introduction

The amount of marine cargo transported has exceeded 10 billion tons in 2016, which is approximately five times that in the 1960s (Ministry of Land, Infrastructure, Transport and Tourism, 2012). It is expected to increase to 15 billion tons in 2050. Maritime transportation, which will become one of the most important types of infrastructure in the future, has been sustaining world economy for decades, and it dominates more than 95% of global cargos (Qinetiq, et al., 2013). It is possible for ships to carry larger quantities of cargo than other modes of transport, despite slower speeds. A ship's performance is strongly influenced by weather conditions including waves, winds, currents, etc. These conditions may delay transportation or jeopardize the safety of the ship. From environmental aspects, the energy efficiency design index (EEDI), which has been in effect since 2012, gives various changes to the ship design to reduce gas emissions (DNV-GL, 2016). The international maritime organization (IMO) also issued the ship energy efficiency management plan (SEEMP) and the energy efficiency operational indicator (EEOI) to achieve environmental-friendly transportation through improved ship operations (Prpić-Oršić, et al., 2012). Although factors related to ship operations has been relatively depending on empirical techniques, a theoretical method is required to optimize these factors. Optimal ship routing is one such methodology to optimize factors including voyage time, fuel consumption, gas emissions, etc. There have been many studies on optimal ship routing since the 1950s (Hanssen et al., 1960; Hagiwara, et al., 1997; Maki, et al., 2011; Lin, et al., 2013). In these studies, the evaluation of speed loss in rough seas has been pivotal for the method's accuracy. Studies have already indicated that speed loss consists of natural and deliberate speed reductiones (Naito, et al., 1979; Faltinsen, 1993). Natural speed loss is caused by the dynamic relation between propulsion and resistance, which includes the added resistance due to waves and winds. Deliberate speed reduction is caused by intentional human operations aimed at preventing damage to ship hulls or main engines, etc. In seakeeping theory, many studies on the added resistance have been conducted (Kashiwagi, 1991 and 1992; Faltinsen et al., 1980; Okusu, 1986). There also have been many studies on deliberate speed reduction with proposals of various parameters to evaluate it in the period between 1960s and 1980s (Aertssen, 1967; Aertssen et al., 1972; Ochi et al, 1974; Gerritsma, 1984). However, because of technological limitations of that time, practical data from actual voyages was not available. Those studies were mainly based on field surveys for seafarers instead of on data analysis. In the field of ship maneuvering, methodologies on ship handling at rough seas are empirically explained (Honda, 1980). It includes deliberate speed reduction and steering, which may be constructed from experiences of seafarers. More recently, onboard monitoring and measuring techniques have been developed to enable continuous data collation that can analyze ship performance in various weather conditions. Because gas emission (fuel consumption) varies in rough sea voyages, it becomes important to understand deliberate speed reduction with respect to the EEDI, the SEEMP, and the EEOI. The international towing tank committee (ITTC) defines deliberate speed reduction as one of the important topics in 2018. The criteria for deliberate speed reduction proposed between 1960s and 1980s should be revaluated against contemporary data from practical marine environments. The authors of this paper in a separate study had already

produced the results of performance analysis of the 28,000-DWT-class bulk carrier in the rough seas of the Southern Hemisphere (Sasa, et al., 2017). Hence, the validity of the criteria in this paper is shown with the measured data gathered from some rough sea voyages. Firstly, the validation is studied for vertical and lateral accelerations, roll motion, probabilities of deck wetness, slamming, and propeller racing, which were previously shown as the criteria for calculating deliberate speed reduction. These parameters are usually monitored from the ship bridge. Other parameters are monitored from the engine room to prevent overloading the main engine or damaging machineries. However, there are few studies on the deliberate speed reduction in relation to the engine parameters as the emergency operation in rough sea voyages. Thus, current conditions of engine operations in rough sea voyages are gathered by surveying marine engineers in Japanese shipping companies. Details of speed loss are analyzed both from measured data and survey results. This paper shows that the limiting value of vertical acceleration of a ship at the bridge is suitable to judge the deliberate speed reduction. On the other hand, limiting values of horizontal acceleration and roll motion are not consistent with the measured results. Different patterns were found for probabilities of deck wetness, slamming, and propeller racing, and the speed was intentionally reduced when values became nonzero. The study also shows that the engine parameters were affected by the speed loss. Finally, simple models were constructed to estimate the deliberate speed reduction as the quadratic function of vertical acceleration or pitch motion. These models can be applied to the numerical simulation of speed loss in rough sea voyages for accurate optimal ship routing.

2. Evaluation Parameters for Deliberate speed reduction in Rough Seas

Vertical and horizontal accelerations of the ship tend to increase during rough sea voyages. When vertical or horizontal acceleration increases, work difficulty of the ship crew occurs in the ship's bridge or engine room. If the tides worsen, strongly nonlinear phenomena such as deck wetness or slamming, which pose danger to a ship, may occur. In addition, strengthening of wind waves increases the added resistance. These factors make it difficult to maintain the navigation speed even when the engine power is increased. This is the typical pattern of natural speed loss. Because it begins to overload as the host ship tries to maintain its speed, the main engine is usually maintained at a constant power. Studies related to natural speed loss began since the 1960s and various studies were conducted between 1970s and 1980s in Europe, Japan, etc. Aertssen (1967) analyzed voyage records in rough seas for cargo vessels and discussed the relation among speed loss, slamming, deck wetness, and propeller racing. Ochi et al. (1974) and Kim et al. (1979) proposed vertical acceleration in fore peak as the criteria for estimating deliberate speed reduction in a container ship, and Kitazawa et al. (1975) added to the studies roll motion from the viewpoint of work difficulty. Gerritsma (1984) derived these criteria for naval ships as well. There are many other related studies that propose various criteria for natural speed loss. NordForsk (1987) conducted an extensive survey on rough sea voyage for ship crews and summarized the relevant criteria against a cargo ship, as shown in Table 1.

Table. 1 Criteria of voluntary speed loss

Vertical Acceleration at fore peak (rms)	0.2 g
Vertical Acceleration at bridge (rms)	0.15 g
Lateral Acceleration at bridge (rms)	0.12 g
Roll (rms)	6.0°
Probability of slamming	0.025
Probability of deck wetness	0.05

Limit values of vertical acceleration at the ship's bridge and fore peak, lateral acceleration at the bridge, and roll motion are defined as their root mean square (rms) values. Slamming and deck wetness in terms of probability are evaluated as 2.5% and 5.0%. A ship shifts from the natural speed loss to the deliberate speed reduction if either of them exceeds its limiting value. Because these criteria were derived from the documents or records available at that time, there are few examples that fit long-range, continuous data measured by accurate sensors in actual seas.

Most of the seafarers surveyed were permanent employees of flagships before the 1980s. This implicates that they have been trained to mature their maneuvering technique in rough seas through long-time experience. The actions taken by these employees for ship handling during rough sea maneuvering are summarized below (Honda, 1980):

(1) Sound a warning if the drop rate of air pressure at the ship is 1 hPa per hour. If the drop rate of air pressure is more than 2 hPa per hour, the ship varies its heading for 180° to turn around its course.

(2) Reduce speed as a countermeasure against deck wetness, slamming, hull damage, collapse of cargo, propeller racing, seasickness, etc. for safety of the ship. Reducing the engine power of a ship to a level corresponding to the standby speed when the speed of the ship can no longer be increased beyond standby, even if the engine is operating at full speed and power mode.

(3) Make a decision to slow down with slamming or deck wetness.

(4) Set the relative wave direction at 30–45° from the bow until the Beaufort wind scale is 6–7. A ship should be at the bow quartering sea state because rough sea maneuvering is usually conducted under Beaufort scale 8. The maneuvering difficulty can be seen in head sea state more than the Beaufort scale 9.

(5) Switch from autopilot to manual steering when roll and pitch motions of the ship increase. However, steering angles must be within 20°, repeatedly avoiding large tides to prevent precarious situations that arise with large-angle steering.

Highly skilled maneuvering techniques are required for these ship handling actions. Those criteria could be decided on the premise of skilled seafarers. Ship crews have been replaced by foreign crews who were temporarily employed after the 1990s, which makes academic operating systems such as optimal ship routing a necessity. It is also necessary to validate the criteria for current seafarers to construct an accurate optimal routing system.

3. Survey of Engine Operations in Rough Sea Voyages

Some parameters have been proposed in the previous section to evaluate deliberate speed reduction, all of which can be experienced in the ship's bridge. Machinery parts of the main engine and shaft are also influenced by the rough sea conditions, and it is necessary to know the engine operation related to tackling the rough sea condition. However, there are few studies focused on the relation between speed loss and engine parameters. Some intentional operations such as engine speed could be seen in the measured data. It is necessary to find out the operational limits for marine engineers, whether they have their own standards or not. Thus, a nationwide questionnaire on current safety operations and standards in rough sea voyages for marine engineers was conducted. Questionnaires were sent to 140 Japanese shipping companies, and nearly half of them (71 companies) responded. The main questions are shown in Table 2, analyzing which revealed some patterns.

Table 2 Questionnaire on main engine operation status during rough sea voyages

Q1	Please explain the rough sea conditions you have encountered. How often do you encounter rough waves (per month or per year)? What sea areas did you venture and what were the wave conditions on those occasions
Q2	Please explain speed loss in rough seas (How does the ship speed drop to the navigational speed?) Is navigation speed generally reduced to cut fuel consumption?
Q3	Please explain the main engine controls during rough seas. What parameters do you monitor to maintain performance of the main engine? (Multiple parameters available)
Q4	How do you define the criteria for parameters in Q3 from the viewpoint of performance or safety maintenance? (Multiple answers available)
Q5	When do you decide to change the settings of the engine controls, if the monitoring parameters approach the criteria?

Responders are classified as shown in Table 3. As shown here, domestic ferries and cargo vessels are the main responders. The types of propulsion systems is different for ferries and cargo vessels, which are controllable pitch propeller (CPP) and fixed pitch propeller (FPP). The analyzed results of the answers to Q1–Q5 are summarized in Figures 1-5.

Table 3 Classification of responders in questionnaire

	0–5,000 GT (%)	5,000–10,000 GT (%)	10,000–15,000 GT (%)	Greater than 15,000 GT (%)
Ferry	27	6	10	8
Tanker	17	0	0	0
Cargo Ship A	12	8	0	0
Cargo Ship B	2	0	0	10

(Note) Cargo Ship A is a domestic-trade ship; Cargo Ship B is a foreign-trade ship

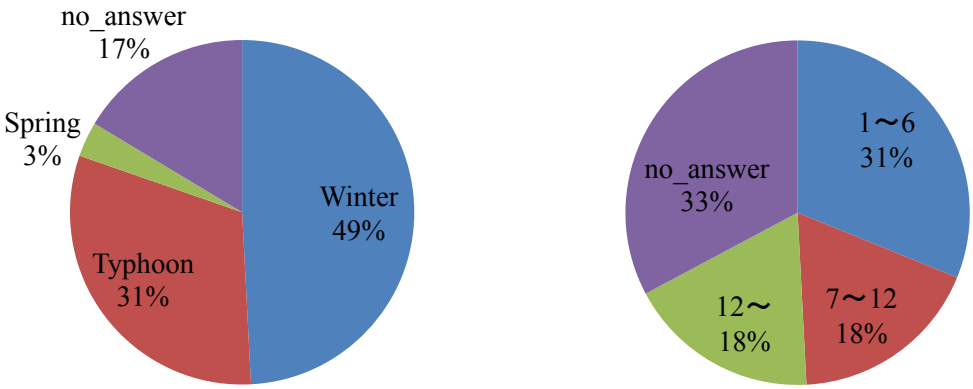

Figure 1 Season and frequency of rough sea voyages

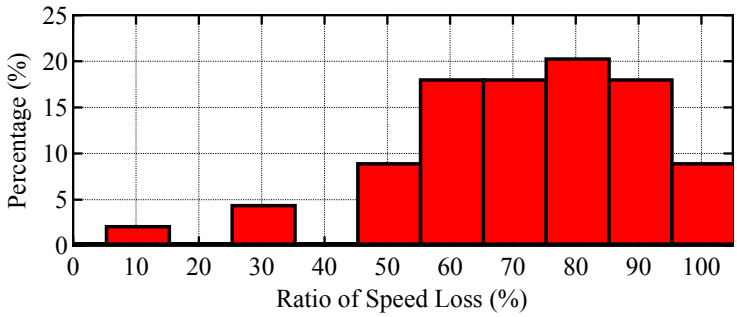

Figure 2 Distribution of speed loss in rough sea voyages

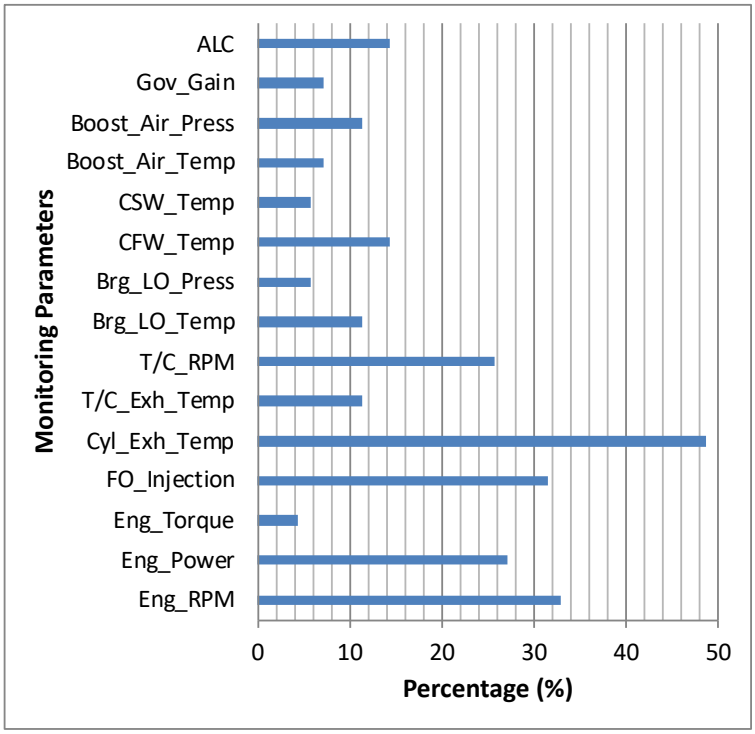

Figure 3 Monitoring parameters in rough sea voyages

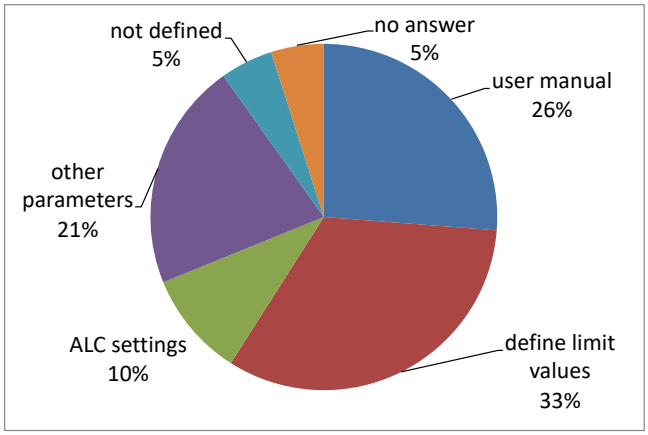

Figure 4 Setting of limiting values in emergency operations for engines

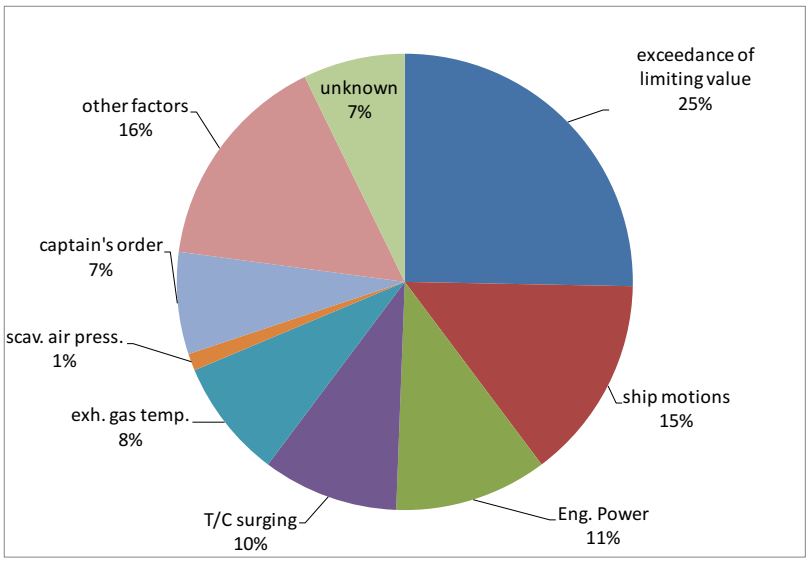

Figure 5 Division of time for deciding engine operations

Figure 1 shows that the responders encountered rough sea conditions mainly in the winter (49%) and in the typhoon season from summer to fall (30%). Frequencies of the encounter are 0–6 times per year (31%), 7–12 times per year (18%), and more than 12 times per year (18%), etc. This means that nearly 20 percent of responders experienced rough sea voyages at least once a month. Many ships reduced their speed as 60–90% of the navigation speed in Figure 2. There are around 15 parameters marine engineers monitor during rough sea voyages in Figure 3. The main monitoring parameters are the exhaust temperatures of cylinders (48%), engine speed (33%), fuel injection (pump mark) (32%), engine power (27%), revolution of blades in the turbocharger (26%), etc. Other parameters are cooling fresh water temperature (14%), boost air pressure (11%), and automatic load control (ALC) for ships with CPP (14%). The resistance increases at the propeller due to external forces, and it is transferred from the shaft to the main engine. In these harsh weather conditions, the ship performance worsens and the phenomenon of engine surging may also be triggered. Under such a situation, the engine speed

cannot be maintained and is actually very low. This situation causes incomplete combustion in the main engine and the rising of exhausted gas temperatures. In rough sea voyages, the airflow between the main engine and turbo charger may be reversed unless the engine speed is reduced. This is referred to as the surging phenomenon. Firstly, fuel injection usually is shifted from automatic to manual control to reduce the volume of fuel injected. The purpose of this operation is to gradually reduce the engine speed, lowering engine load through deliberate speed reduction—it is reasonable to monitor these parameters for this purpose. In Figure 4, the limiting value is decided from the performance curves of manufacturers (26%), the empirical values defined from their experience (33%), and the ALC (10%) for ships with CPP. Figure 5 shows that the slow down operation is decided when the monitoring value approaches the limiting value in the performance curves (25%), ship motions or sea conditions become worse (15%), the engine power approaches the criteria (11%), the possibility of surging increases (10%), the temperature of exhaust gas increases (8 %), communication with the captain (7 %), etc. Although many parameters are monitored in the engine room, the final decision of deliberately decreasing speed is not made by the marine engineers alone. This point is further surveyed through a visiting interview with a Japanese shipping company in June 2018. The main points of the survey are summarized below.

(1) The employment of seafarers has changed since the 1980s, and skilled seafarers with more experience are fewer in number today. The maneuvering over rough seas discussed in section 2 cannot be applied for many of the current seafarers. Scientific support such as optimal ship routing must be simultaneously used in the ship operation.

(2) The chief engineer usually directs the captain to lower the loads when the engine power increases. The captain then makes a decision about the emergency operation to be implemented by considering all the situations.

(3) It is ideal to reduce the engine speed (ship speed) right before entering turbulent waters. It is said that the pitch motion, especially in the container ship, tends to reduce its ship speed. The steering should be avoided as much as possible, especially in the ballast condition.

(4) Marine engineers monitor various parameters and report any abnormalities to the ship's bridge. However, they do not have the authority to make decisions independently. The captain takes the final decision on the operation.

These comments are mostly consistent with the questionnaire result. Therefore, each parameter shown in Table 1 will be validated and, at the same time, the engine parameters will be analyzed in the next section.

4. Validation of Survey Results with Onboard Measured Data

4.1 Onboard Measured Data in Actual Sea

The validity of parameters discussed in previous sections is considered for the measured data of the 28,000-DWT-class bulk carrier in actual seas (Sasa, et al, 2015; Sasa, et al., 2017; Lu, et al., 2017). The measurement was conducted from July 2010 to August 2016, with periods of missing data in between because of mechanical troubles. Main dimensions of the 28,000-DWT bulk carrier are shown in Table 4.

Table 4 Main dimensions of 28,000-DWT-class bulk carrier

Length between perpendiculars	160.4 m
Breadth	27.2 m
Draft (fully loaded)	9.82 m
Dead weight	28,189 t
Navigation speed	14.0 knots

The measurement system consists of the voyage data recorder and the engine data logger, and these data are transmitted to the integrated bridge satellite system (IBSS) for establishing communication between ship and ground station. Here, two laptops are connected with the IBSS to collate navigation data such as position, speed, course, steer angle, wind direction and speed, etc. and engine data such as engine speed, shaft thrust, engine power, exhaust gas temperature, revolution of blades in the turbocharger, etc., which are recorded every 1.0 s. Ship motions and accelerations are measured by an inertial measurement unit (NAV440) that records measured results every 0.1 s. It is necessary to estimate the wave conditions, which are numerically estimated by Wave WATCH III, a third-generation global wave model (Tolman, 2002). The model computes for the global region using the two-way nesting technique. The condition is defined by the outer region of 0.5° and the inner region of 0.1°. Global wind information is required for the computation with two types of reanalysis database, NCEP-FNL, distributed from the NCEP (National Centers for Environmental Prediction) (Kalnay et al., 1996), which is based in the USA; And the ERA-interim, distributed from the ECMWF (European Centre for Medium-Range Weather Forecasts) (Dee, et al., 2011), which is based in Europe. Three types of wind data are defined as the input of Wave WATCH III as shown in Table 5.

Table 5 Three kinds of wave estimation

Method	Database	Detail of wave estimation
NCEP	NCEP-FNL	Linear interpolation from 1° to 0.5° and 0.1°
ERA	ERA-interim	Linear interpolation from 0.75° to 0.5° and 0.1°
WRF	NCEP-FNL	Wind distributions are numerically simulated by the atmospheric model, WRF (Input: 1°, Output: 0.1°)

The NCEP method defines wave estimation using NCEP–FNL with a spatial resolution of 1.0° and interpolates linearly to 0.5°, and 0.1°. The ERA method defines wave estimation using ERA-interim with a spatial resolution of 0.75° and interpolates linearly to 0.5° and 0.1°. The WRF method defines wave estimation using wind conditions computed by the WRF (Shamarock, et al., 2008), the regional air model, for the NCEP–FNL. Three types of wave information are used to calculate probabilities of deck wetness, slamming, and propeller racing, respectively. The ship trajectory from February to October 2013 is shown in Figure 6.

Figure 6 Ship trajectory from February 2013 to October 2013

As shown in the figure, the bulk carrier has been mainly cruising in the Southern Hemisphere through the Indian Ocean, the Atlantic Ocean, the Tasman Sea, and the Pacific Ocean. Three rough sea voyages are selected for the validation, as shown in Table 6.

Table 6 Details of rough sea voyages

Case	Year and Date	Sea Area
A	June 1–3, 2013	Off the coast of South Africa, Indian and Atlantic Oceans
B	June 14–16, 2013	Off the coast of South America, Atlantic Ocean
C	March 14–17, 2013	Off the coast of Australia and New Zealand, Tasman Sea

As shown in Figure 6, cases A and B are on the same trajectory from China to Uruguay, with the half-loaded condition. The ship encountered rough seas offshore the African and South American continents. Case C embarks on a rough sea voyage from Australia to New Zealand with the ballast condition. Estimated wave heights at the ship positions in each case are shown from Figures 7–9 (Lu, et al., 2017).

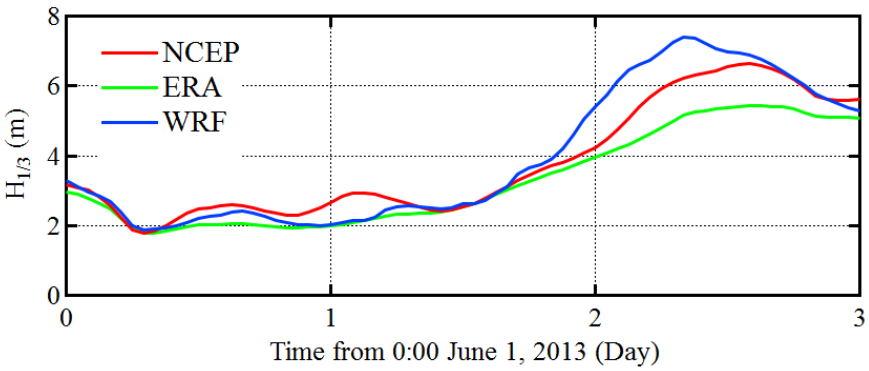

Figure 7 Variation of estimated wave height in June 1–3, 2013

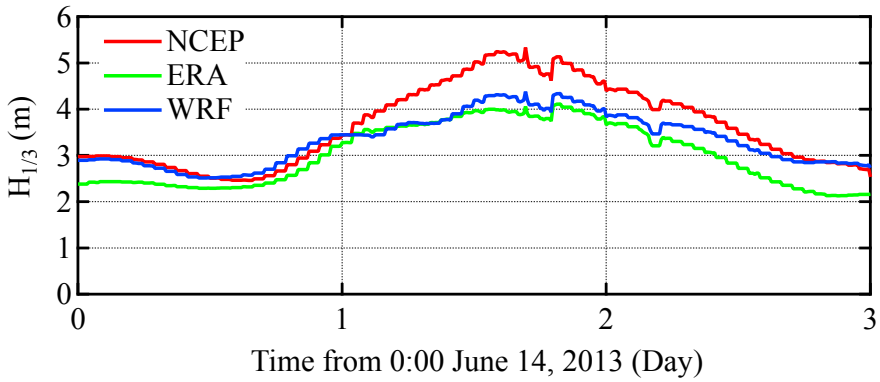

Figure 8 Variation of estimated wave height in June 14–16, 2013

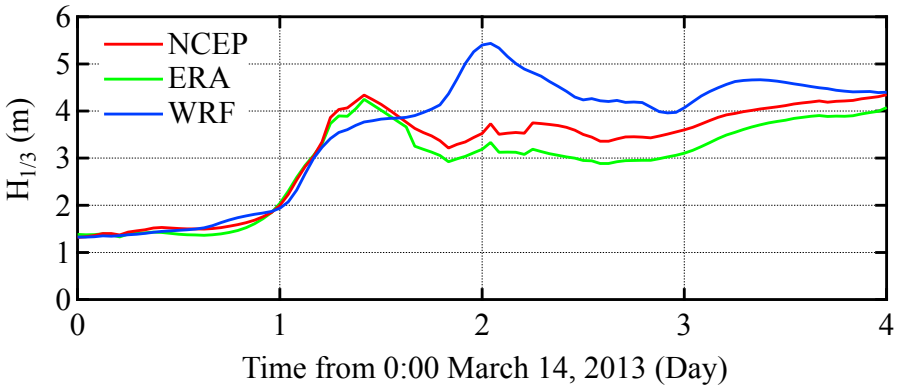

Figure 9 Variation of estimated wave height in March 14–17, 2013

The maximum value of significant wave height for Case A in June 3 is 5–7 m, and this is the roughest wave condition among the three cases. Wave heights for Case B in June 15 are 4–5 m. For Case C from March 15 to March 17, they are 3–5 m, and the wave direction varies from head sea state to following state. Larger ship motions in pitch and roll directions are generated with significant speed losses, and detailed situations are analyzed for those cases.

4.2 Analysis Method of Measured Data

If a ship encounters turbulent sea conditions, the added resistance is considered as a function of wave height, wave period, wave direction, wind speed, and wind direction. The added wave resistance is a time-averaged value of the longitudinal second-order hydrodynamic force, which can be analyzed by the seakeeping theory (Kashiwagi, 1991 and 1992). The ship speed is then decided as a relation of the following equations. It is basically discussed for regular waves in frequency domain. In case of irregular sea state, the ship speed is decided by solving the following equations in frequency and time domain (Sasa, et al., 2017).

$$\beta_V(x_p, y_p, z_r)(1-t)T(n,V) = R_{SW}(V) + R_{AW}(\chi, \omega, H, V) + R_{AWD}(\varphi, U, V), \quad (1)$$

$$\left(M + m_{11}(\omega)\right)\frac{dV}{dt} = \beta_V(x_p, y_p, z_r)(1-t)T(n,V) - R_{SW}(V) - R_{AW}(\chi, \omega, H, V) - R_{AWD}(\varphi, U, V) \ , \quad (2)$$

where β_V is the thrust deduction factor due to ventilation (Smogeli, 2006), t is the thrust deduction fraction, which reflects the ship's increase in resistance in calm waters due to working propulsion units such as the propeller, T is the shaft thrust, n is the revolution of the main engine and shaft (no reduction gears in the ship), V is the ship's speed, R_{SW} is the resistance of still water, R_{AW} is the added resistance from waves, χ is the relative wave direction, ω is the encounter frequency, H is the significant wave height, R_{AWD} is the added resistance due to winds, φ is the relative wind direction, and U is the wind speed, M is the ship's mass, and m_{11} is the added mass in surge mode. If wave conditions become rougher, the value of β_V will decrease and the values of R_{AW} and R_{AWD} will increase remarkably. In harsh sea conditions, the thrust deduction is also evaluated in the following method (Faltinsen, et al., 1980).

$$t = \frac{2}{1+\sqrt{1+C_T}}\frac{w_P}{1-w} \ , \quad (3)$$

where, w is the effective wake, w_P is the potential wake, and C_T is expressed as

$$C_T = \frac{2T(n,V)}{\rho V_d^2 \pi R^2} \ , \quad (4)$$

where, ρ is the water density, V_a is the speed of advance, R is the radius of propeller. If the speed of advance decreases, the value of t also decreases. Wave series have different amplitudes and periods for each component. The added resistance in irregular waves can be approximated as a series of regular waves with different amplitudes and periods. Each regular wave is a combination of two neighboring waves of half wave length. The zero-up cross method is used to analyze the wave series. Eq. (2) is numerically solved using the fourth order Runge-Kutta method. The speed loss can be estimated in Eqs. (1) and (2). In Eq. (1), the ship's speed V should be decreased to reduce R_{SW} for the right-hand term to be equivalent to the left-hand term, when the added resistances increase in rough sea conditions. Therefore, the ship's speed, V, is controlled to decrease with the revolution, n. This is the typical mechanism of speed loss, and the deliberate speed reduction is also added here. An inertial measurement unit is installed at the ship's bridge and is evaluated as the root mean square.

$$\ddot{z}_B = \sqrt{\frac{1}{N}\sum_{i=1}^{N} \ddot{z}_{BR}(i)^2}, \tag{5}$$

$$\ddot{y}_B = \sqrt{\frac{1}{N}\sum_{i=1}^{N} \ddot{y}_{BR}(i)^2}, \tag{6}$$

$$\ddot{x}_B = \sqrt{\frac{1}{N}\sum_{i=1}^{N} \ddot{x}_{BR}(i)^2}, \tag{7}$$

$$X_{RS} = \sqrt{\frac{1}{N}\sum_{i=1}^{N} X_{RBR}(i)^2}, \tag{8}$$

where, $\ddot{z}_B$, $\ddot{y}_B$, and $\ddot{x}_B$ are the root mean square values of the vertical, lateral, and longitudinal accelerations, X_{RS} is the root mean square of roll motion, $\ddot{z}_{BR}(i)$, $\ddot{y}_{BR}(i)$, and $\ddot{x}_{BR}(i)$ are the i-th amplitudes of accelerations in the vertical, lateral, and longitudinal directions, $X_{RBR}(i)$ is the i-th amplitude of roll motion, N is the amplitude number. The volume of data should be large enough to obtain statistically stable results. The relative wave direction should be constant in each data unit. According to the former research (Sasa et al., 2017), the relative wave direction varies every 10-30 min. in rough sea conditions. Therefore, the data unit length is defined as 10 min. Statistical accuracy is shown to be almost constant for this data period (Lu, et al., 2017). The amplitudes are obtained from measured time series using the zero-up crossing method. Probabilities of deck wetness, slamming, and propeller racing are defined below.

$$P(DW) = P\left(z_r(FP) > h_f\right), \tag{9}$$

$$P(S) = P\left(z_r(FP) < -d_f \ \cap \ \dot{z}_r(FP) > \ v_c\right), \tag{10}$$

$$P(PR) = P\left(z_r(AP) > -d_p\right), \tag{11}$$

where, $P(DW)$, $P(S)$, and $P(PR)$ are the probabilities of deck wetness, slamming, and propeller racing, respectively, h_f is the vertical height between the water surface and the deck, d_f is the draft forward of the ship, and d_p is the vertical distance between the water surface and the propeller. If the water surface is below one-third of the propeller diameter from the top, then propeller racing will occur. $z_r(FP)$ and $z_r(AP)$ are the relative water surfaces in the fore peak and aft peak, defined as:

$$z_r(FP,t) = X_H(t) + \ell'_x X_P(t) + \zeta_0(t), \tag{12}$$

$$z_r(AP,t) = X_H(t) - \ell''_x X_P(t) + \zeta_0(t), \tag{13}$$

where, $X_H(t)$ and $X_P(t)$ are heave and roll motions, $\zeta_0(t)$ is the free surface of water elevation under the ship, ℓ'_x and ℓ''_x are the longitudinal distances from the center of gravity to the fore peak and the aft peak, respectively. The inertial measurement unit does not output the heave motion, which is obtained as follows.

$$X_H(t) = \sum_{i=1}^{NF} \sqrt{2S_H(\omega_i)\Delta\omega}\cos(\omega_i t - \epsilon_i), \tag{14}$$

where, $S_H(\omega)$ is the frequency spectrum of heave motion, ω is the angular frequency, ε is the phase, and NF is the number of wave components. The spectrum of heave motion can be obtained as the integration of vertical acceleration at the center of gravity.

$$S_H(\omega) = \frac{S_Z(\omega)}{\omega^4}, \tag{15}$$

where, $S_Z(\omega)$ is the frequency spectrum of vertical acceleration at the center of gravity, and its value is set as a constant of $S_Z(0.125)$ for $\omega < 0.125$ (rad/s). The free surface, $\zeta_0(t)$, is defined as:

$$\zeta_0(t) = \sum_{i=1}^{ND}\sum_{j=1}^{NF} \sqrt{2D_W(\omega_i,\theta_i)\Delta\theta\Delta\omega}\cos(\omega_i t - \epsilon_i), \tag{16}$$

where, $D_W(\omega, \theta)$ is the directional spectrum of the wave, which is obtained from the wave simulator, Wave WATCH III. In Eq. (17), v_c is the vertical speed of impact on the water surface with the bow part of ship. Ochi's formula is used here as:

$$v_c = (0.08 \sim 0.11)\sqrt{gL}, \tag{17}$$

where, g is the acceleration due to gravity and L is the length of the ship. Those parameters are computed every 10 min of the measured data and are compared with the criteria given in Table 1. Parameters in the engine room are also analyzed as a 1-min average value. Relations of these parameters with deliberate speed reduction are

analyzed in later subsections.

4.3 Analyzed Results of Onboard Measured Data

Measured data of ship motions, accelerations, the ship's speed, etc. are analyzed and compared with the criteria of earlier studies in each case.

(1) Case A

Variations of $\ddot{z}_B$, $\ddot{y}_B$, $\ddot{x}_B$, and X_{RS} are analyzed in June 1–3, 2013, as shown in Figure 10. The criteria for each parameter are represented by the red line in the figure. To compare, variations of the ship's speed over the ground and engine speed per minute (in rpm) are shown in Figure 11.

In Figure 10, the value of $\ddot{z}_B$ increases significantly from approximately 40 h and exceeds the criteria, 0.15g. The value of $\ddot{x}_B$ also approaches the criteria of lateral acceleration, 0.12g, from approximately 40–50 h. This tendency is similar to that of the vertical acceleration, with pitch motion significantly influencing it. Values of lateral acceleration and roll motion exceed the criteria, 0.12g and 6°, in most of the periods. As shown in Figure 11, the ship's speed increases once to 18 knots in 12–20 h before the speed loss occurs. This might be influenced by the Agulhas Current, which is a strong current off the coast of South Africa. The ship reduces its speed from 14 knots to 12 knots to save fuel. The marginal speed loss can be seen at approximately 30 h, while the engine speed is still constant. The reductions in the ship's speed and engine speed obviously occur at the same time after 40 h, which is almost the same time at which the vertical acceleration in the bridge exceeded the criteria of 0.15g. It can be assumed that the speed loss from 24 to 40 h is natural and that after 40 h is deliberate. However, the lateral acceleration and the roll motion are not consistent with the timing of deliberate speed reduction. The increased steering after 40 h helps maintain the ship's course and it sail in head waves. Although this maneuvering leads to an increase in fuel consumption, the roll motion can be effectively controlled. They also increase remarkably after 60 h and have very similar variations, meaning that a time difference of 20 h can be observed between the vertical and lateral motions. It is thought that measured results agree with the criteria in longitudinal motions but not with that in lateral motions. Figure 12 shows the total rudder angles in port and starboard as an integrated value per minute, and the averaged variation of ship's heading. The amount of steering increased once at approximately 36 h, which is a few hours before the significant reduction in the ship's speed and engine speed. It increases after 40 h, and the possibility of intentional steering can be thought to vary with the relative wave direction. However, the details are still unclear.

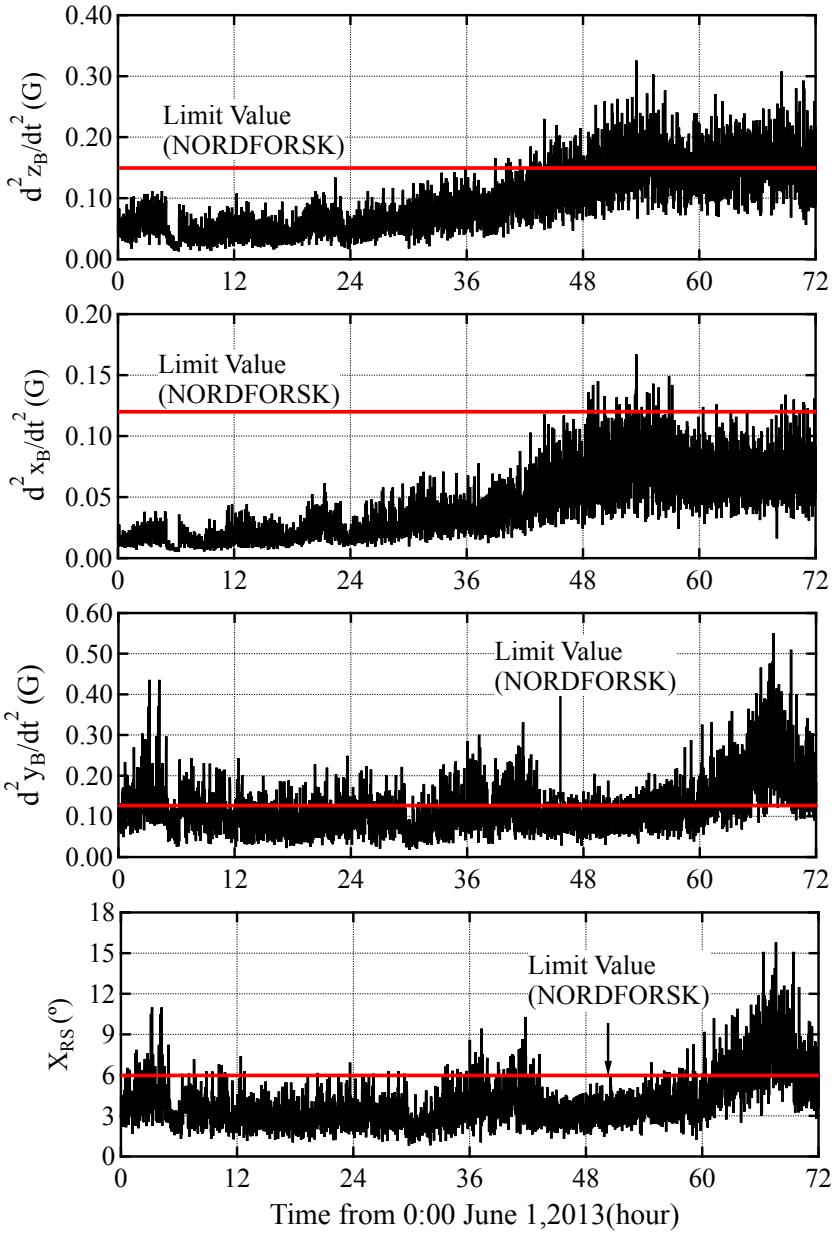

Figure 10 Variations of vertical, longitudinal, lateral accelerations, and roll motion (Case A)

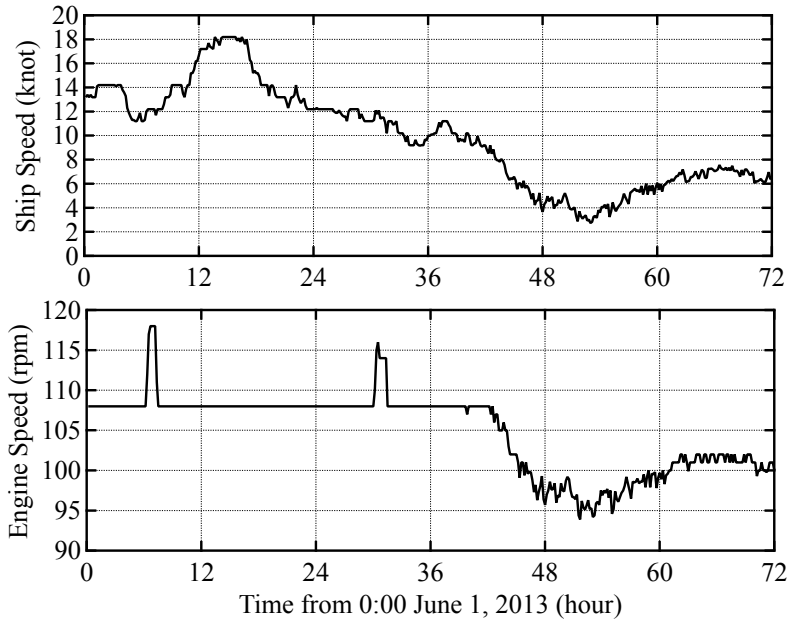

Figure 11 Variations in ship's speed and engine speed (Case A)

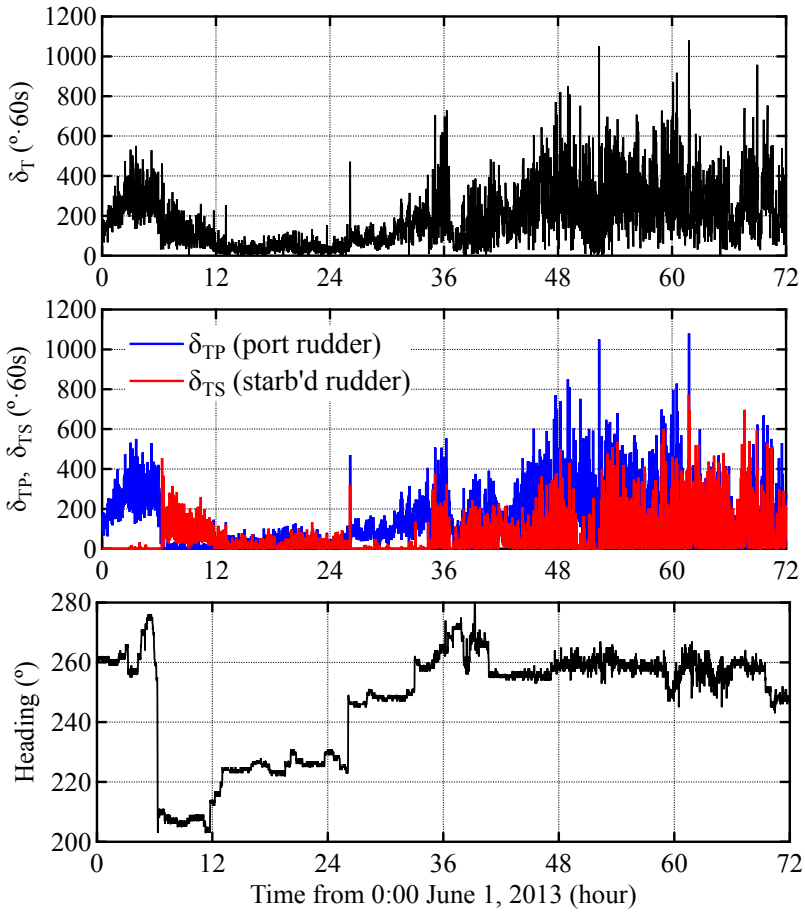

Figure 12 Variations in total rudder angles and ship's heading (Case A)

Relative water surfaces at the fore peak and the probabilities of deck wetness are summarized in each wave estimation method, ERA, NCEP, and WRF, as shown in Figure 13.

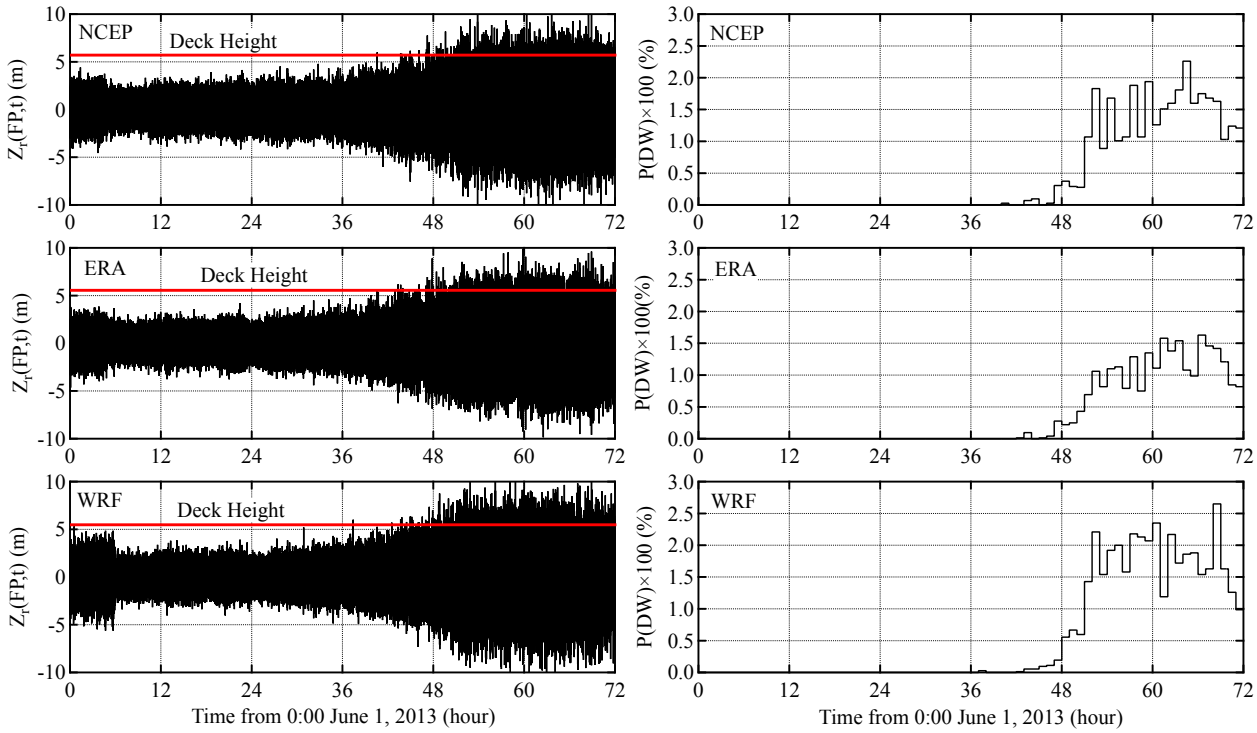

Figure 13 Variations in relative water surface and deck wetness probability (Case A)

The relative water surface is the smallest in the ERA method and the largest in the WRF method. Red lines in the figure indicate the height of the deck from the water surface (5.57 m), and the deck wetness can occur if the relative water surface exceeds this height. The probability is evaluated as the number of exceedances per hour. The probability begins to yield positive values after 40 h for three methods, and this is the same timing of the reduction of the ship's speed and engine speed, and the exceedance of the criteria of vertical acceleration. The probabilities are 1–3% after 50 h, which is still less than the criteria of deck wetness (5%). The criteria are inconsistent with the measured result of speed loss for Case A. The probability of slamming is computed as shown in Figure 14.

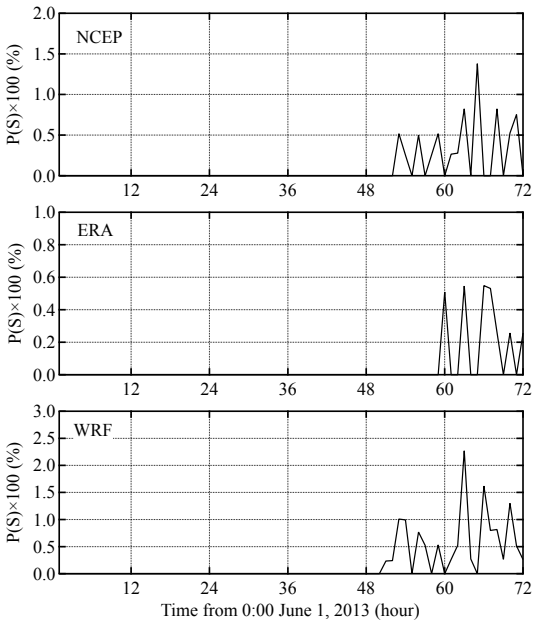

Figure 14 Variations in probability of slamming (Case A)

The probability is extremely low, the maximum value is 0.5–2.0% at approximately 50 h, because the ship is in the half-loaded condition. There are no results exceed the criteria of slamming, 2.5 % for Case A. The relative water surface and the probability of propeller racing is computed as shown in Figure 15.

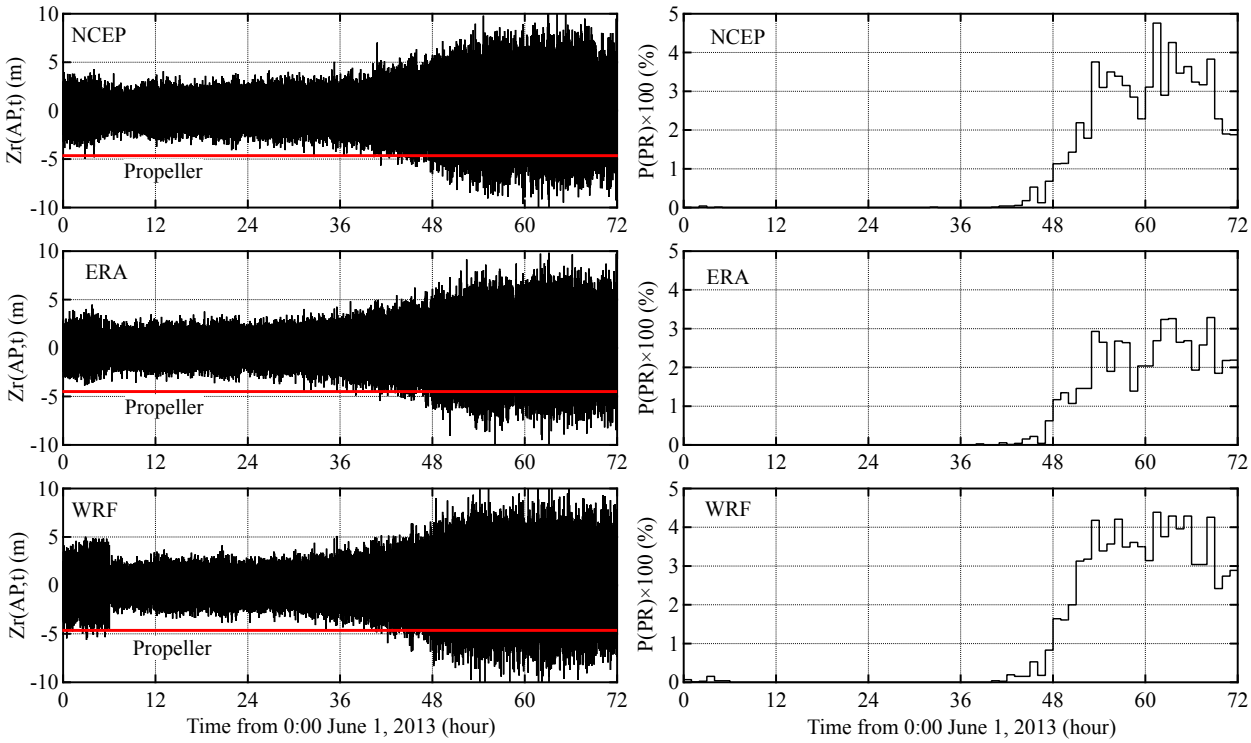

Figure 15 Variation in relative water surface and probability of propeller racing (Case A)

Red lines in the figure show the vertical distance between the water surface and the height of one-third of the propeller diameter from the top, d_p. The propeller racing begins at approximately 40 h, which is almost the same timing as the occurrence of deck wetness, and the lowering of the ship's speed and engine speed. These results indicate that the ship captain intentionally reduces its speed at the start of deck wetness and propeller racing, and do not agree with the probabilities shown in Table 1. This is consistent with the survey results in section 2.

(2) Case B

Variations in $\ddot{z}_B$, $\ddot{y}_B$, $\ddot{x}_B$, and X_{RS} are analyzed for June 14–17, 2013, as shown in Figure 16. Variations in the ship's speed and engine speed for the same period are summarized in Figure 17.

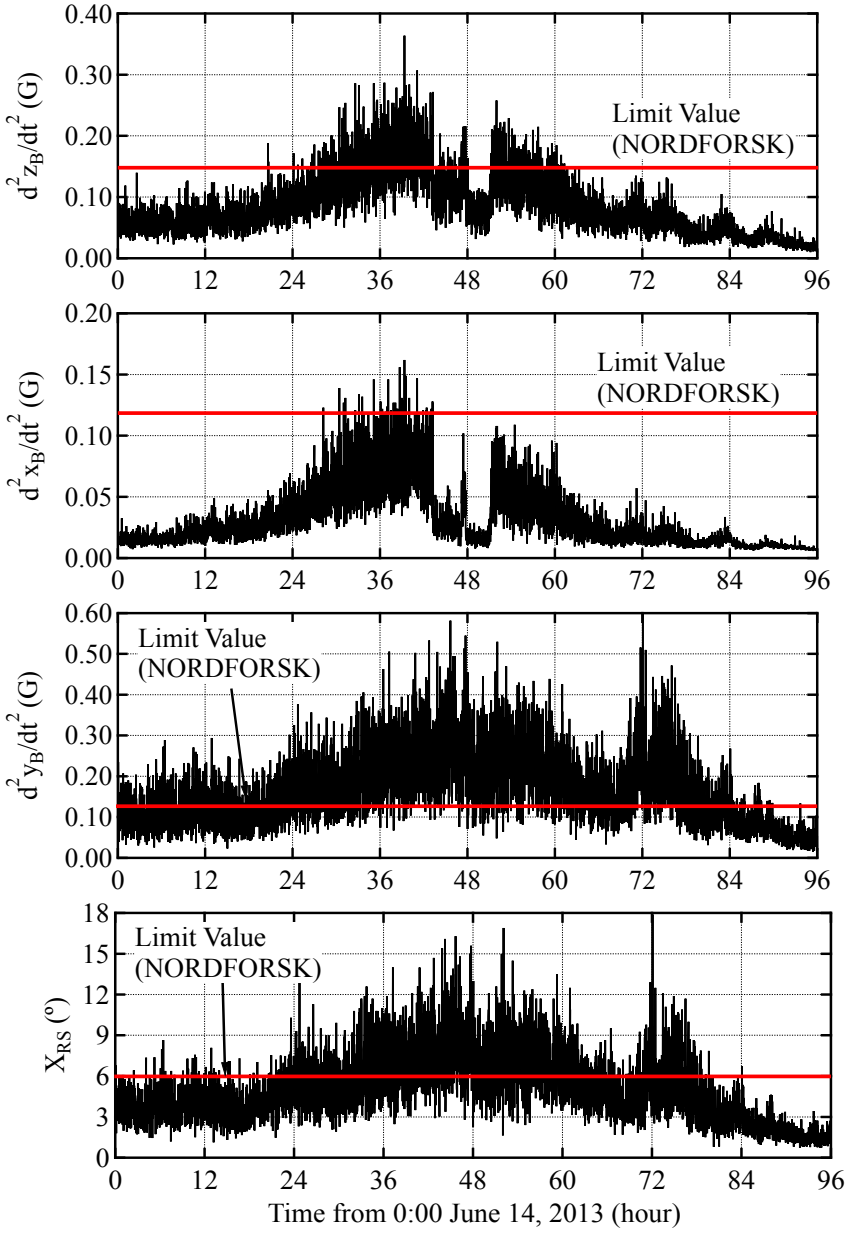

Figure 16 Variations in vertical and horizontal accelerations, and roll motion (Case B)

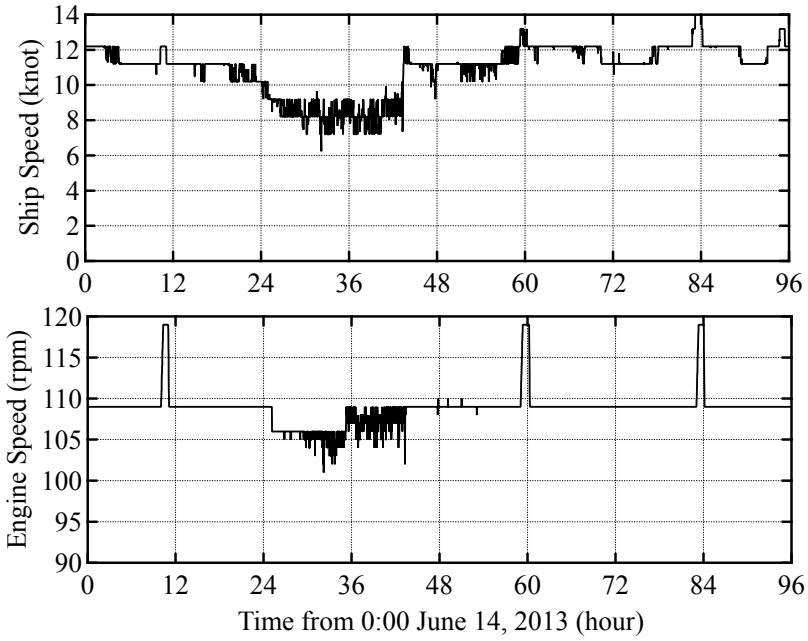

Figure 17 Variations in ship's speed and engine speed (Case B)

From Figure 16, it is obvious that the value of $\ddot{z}_B$ increases and exceeds the criteria of 0.15g from 24 h, and its maximum value is approximately 0.3g, which is similar to that in Case A. The values of $\ddot{x}_B$ are less than the criteria of 0.12g, while the values of $\ddot{y}_B$ exceed the criteria of 0.12g, during the period. The value of X_{RS} varies at the same timing with the vertical acceleration. The speed loss and reducing engine speed can be observed from 24 h, and they can be seen almost at the same timing. Thus, deliberated speed loss could have occurred from 24 h in this case. The range of speed loss and engine speed is 4–5 knots and 3 rpm, respectively, and they are smaller than those in Case A. It is necessary to consider the reason for the difference of speed loss despite the similar trends of vertical acceleration. Variations of the total rudder angles and the ship's heading are summarized in Figure 18.

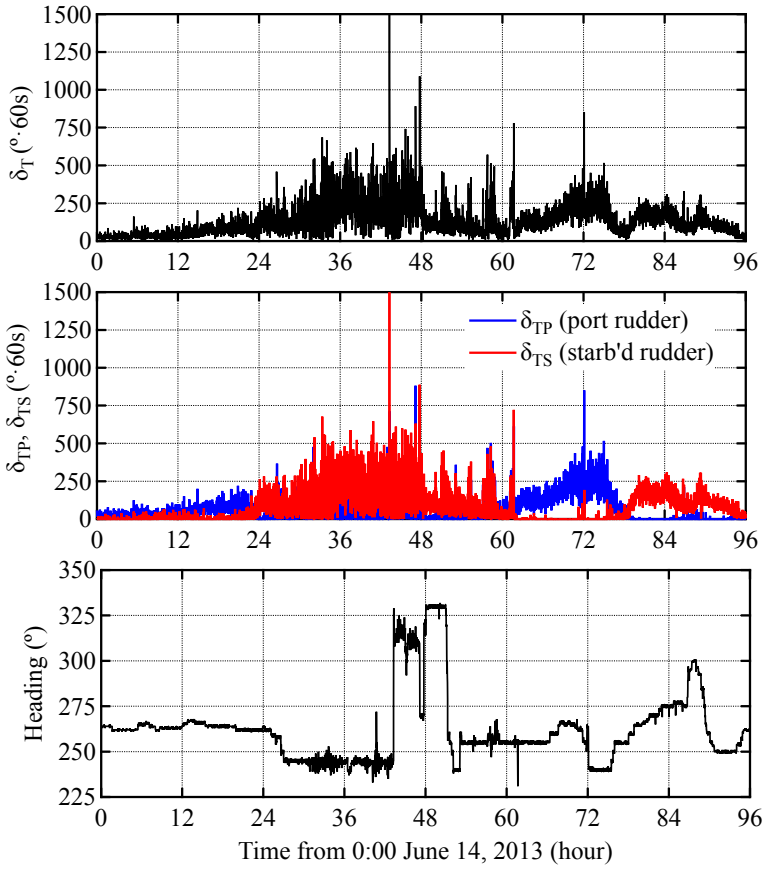

Figure 18 Variation of rudder angles and ship's heading (Case B)

It is obvious that the degree of steering has increased during the period of 24—60 h, and the ship's heading has been varied for 80° from 42—54 h. During this period, it can also be seen that vertical and longitudinal accelerations have decreased significantly, in Figure 16. A description of the difficulty of maintaining the course is recorded in the logbook at that time, which presents the need for an intentional maneuver to avoid the very harsh head sea state, as the vertical motions have been reduced. A strong current exists offshore the South African continent, besides the high tides, which lead the ship with larger steering angles. Larger angles should be avoided for safety, as mentioned in section 2. As a result of this steering, accelerations are significantly reduced, and the ship's speed and engine speed are recovered in the case. Relative water surfaces and probabilities of deck wetness are summarized for three methods, as shown in Figure 19.

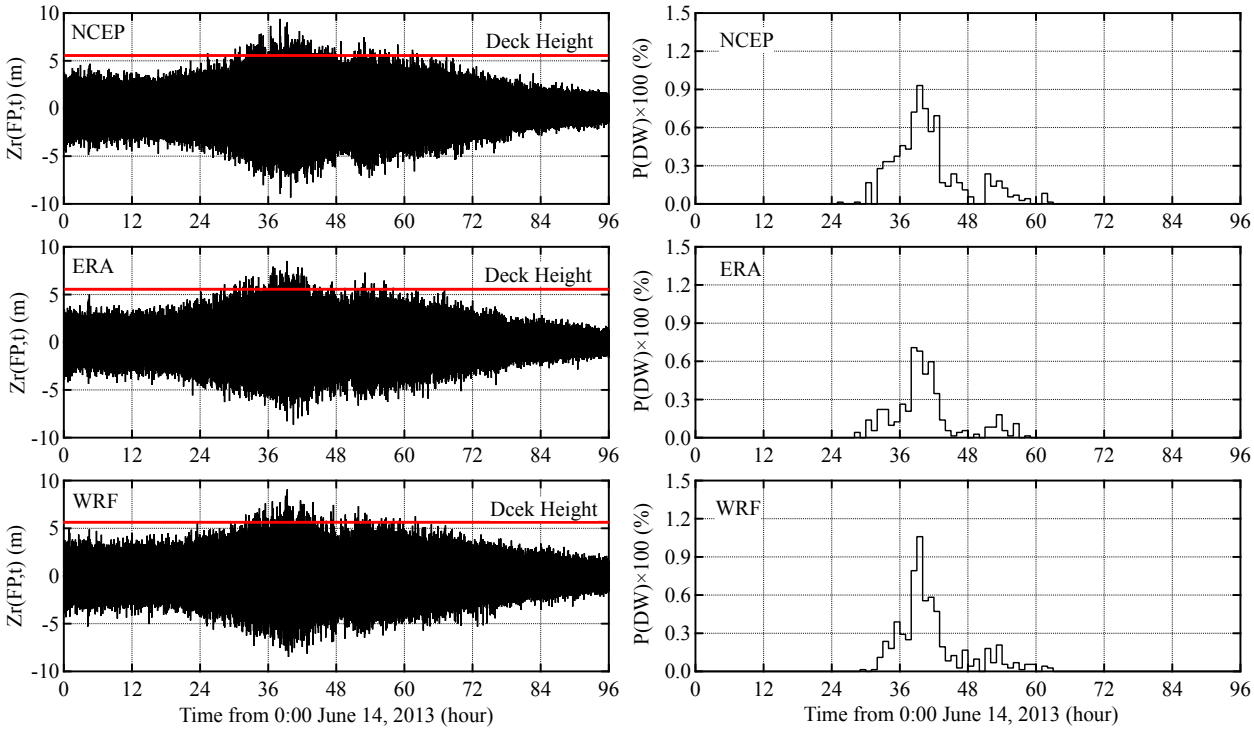

Figure 19 Variations in relative water surface and probability of deck wetness (Case B)

In this case, too, the relative water surface is the smallest in the ERA method and the largest in the WRF method. Probabilities begin to climb above zero from approximately 30 h, which is a few hours after the speed loss has occurred and is the close to the timing of the vertical acceleration, the ship's speed, and the engine speed. However, the probability is around 1% in this case, which is nearly half of that in Case A. The difference of probability may have a relation with the difference of speed loss. Probabilities of slamming for three methods are summarized in Figure 20.

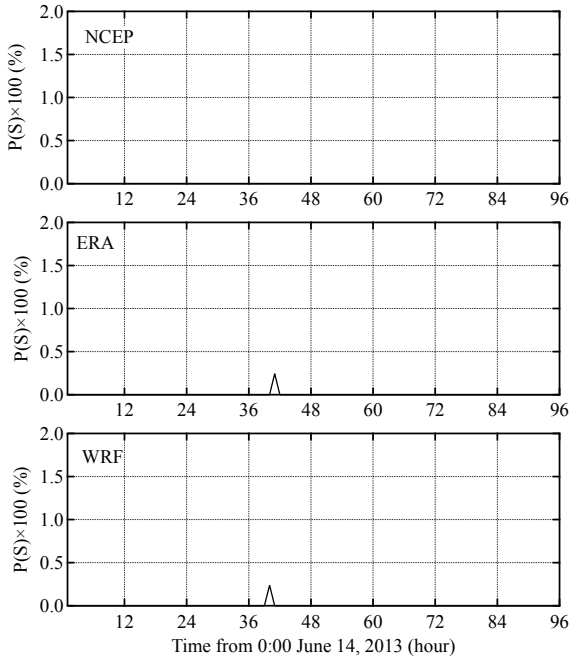

Figure 20 Variations in probabilities of slamming (Case B)

The maximum probability is 0.3%, which means that slamming has not occurred significantly. The relative water surface is less for 2–4 m than those in Case A, which is one of the reasons for the reduced speed loss. Relative water surfaces at the aft peak and probabilities of propeller racing are shown in Figure 21.

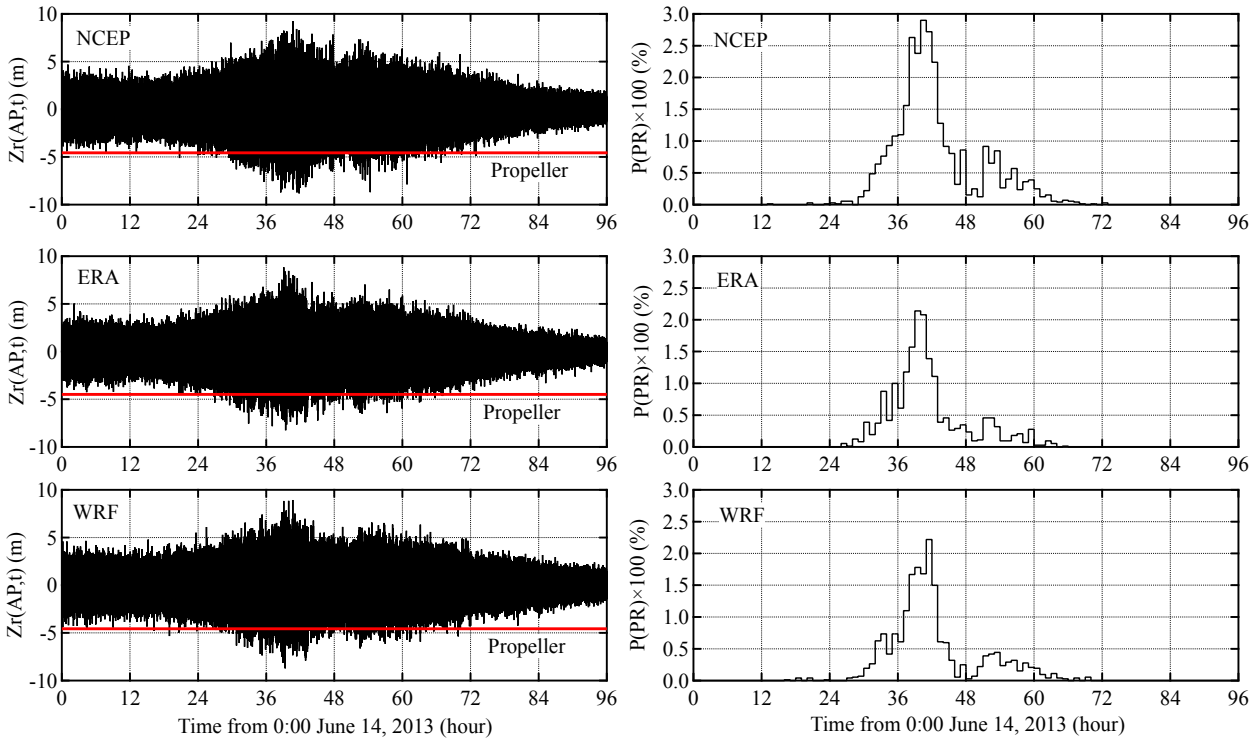

Figure 21 Variation in relative water surface and probability of propeller racing (Case B)

The figure shows that propeller racing also occurs at almost the same time as deck wetness does, which is approximately 24 h and is consistent with the lowering of the ship's speed and engine speed. The probability of propeller racing widely decreases at approximately 40 h, and the lowering of longitudinal motions by varying wave directions strongly contributes to this result. The probability of the propeller racing is 2.0–3.0%, which is lower by 1–2% than those in Case A. A similar tendency is followed by the probability of deck wetness, which can be used for the evaluation of deliberate speed reduction.

(3) Case C

In this case, the ship is in the Tasman Sea between Australia and New Zealand, from March 14–17, 2013. In our previous study (Lu, et al., 2017), low pressure trough exists in the Tasman Sea, with swells from the South Pole. It makes the wave conditions complex and causes the ship to alter its heading repeatedly and irregularly. The loaded condition in this case is a near-ballast one, which is quite different from those in Cases A and B. Variations in $\ddot{z}_B$, $\ddot{y}_B$, $\ddot{x}_B$, and X_{RS} are analyzed for March 14–17, 2013, as shown in Figure 22. Variations in the ship's speed and engine speed are also summarized for the same period, as shown in Figure 23.

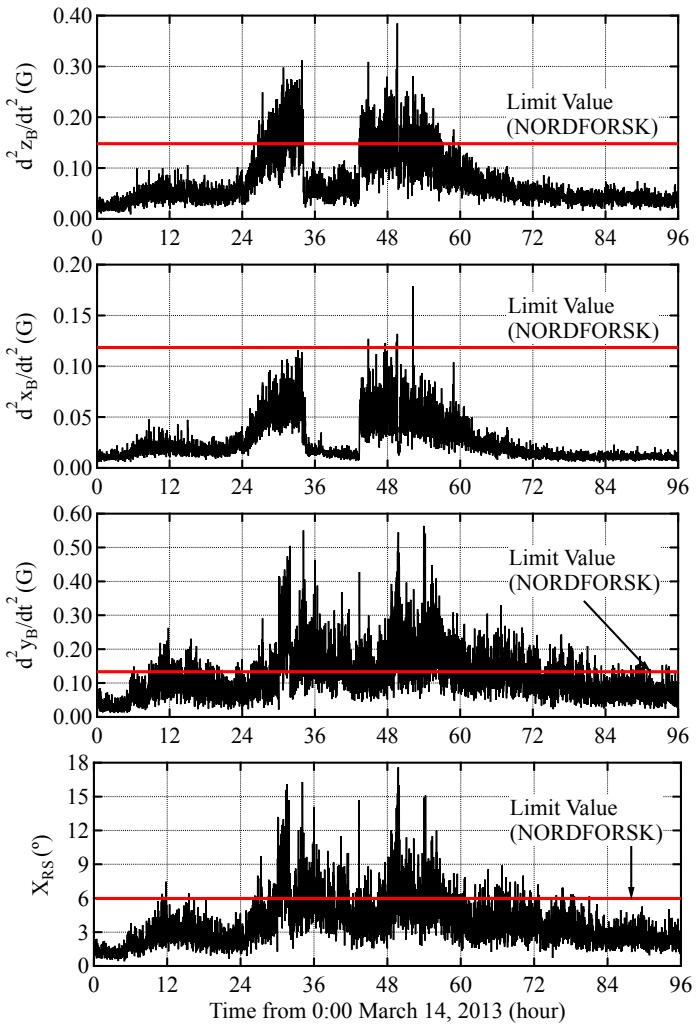

Figure 22 Variations in vertical and horizontal accelerations, and roll motion (Case C)

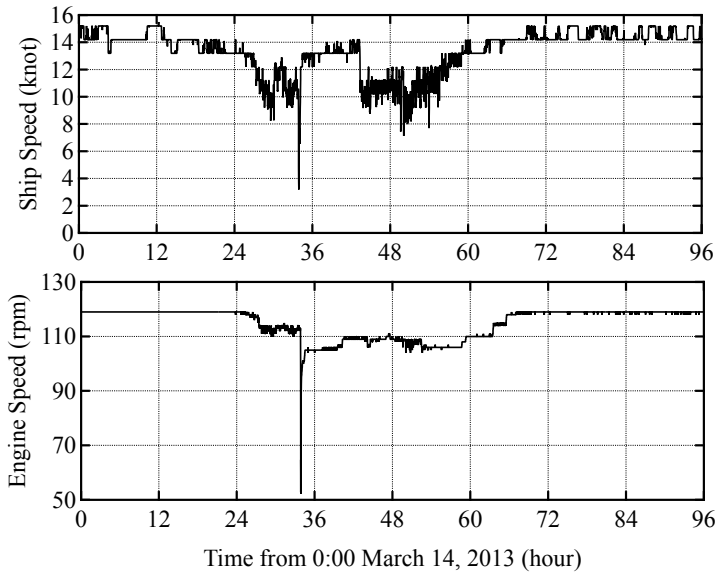

Figure 23 Variations in ship's speed and engine speed (Case C)

Values of $\ddot{z}_B$ and $\ddot{x}_B$ increase remarkably in the time periods of 24–34 h and 40–55 h. After 30 h, the vertical acceleration exceeds the criteria of 0.15g. The longitudinal acceleration follows a similar tendency as that of $\ddot{z}_B$. The lateral acceleration exceeds the criteria, 0.12g, during the period. The roll motion exceeds the criteria of 6.0° in the time period of 24–72 h. It is obvious that the ship's speed and engine speed follow a decreasing trend from 24 h, which is nearly the same time as the vertical acceleration, as shown in Figure 23. These patterns are similar to those in Cases A and B. The ship proceeds at 14 knots initially and slows down to approximately 8 knots. The speed loss in this case is deliberate. Variations in the total rudder angle per minute and the ship's heading are summarized in Figure 24.

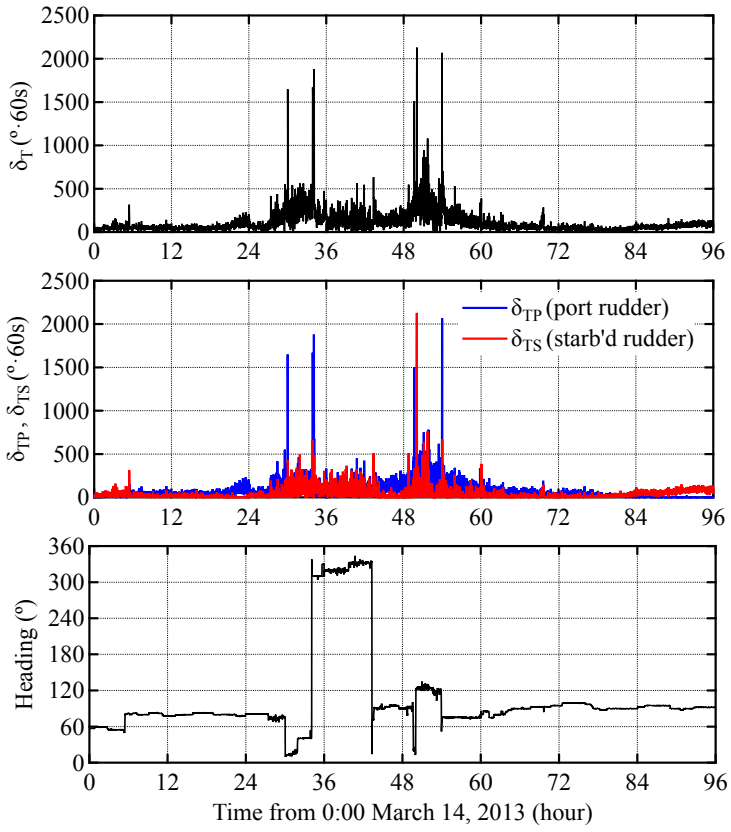

Figure 24 Variations in ship's rudder angles and heading (Case C)

Large steering angles, 1,500–2,000°min, are repeatedly used after 30 h, and this makes the value of $\ddot{z}_B$ decrease in the time period from 34–44 h. However, the value of $\ddot{z}_B$ increases again after 44 h when the ship has altered its course to the East. Although speed loss occurs again in this situation, it must be natural as the engine speed is constant. The abnormal drop in engine speed by more than 60 rpm occurs at approximately 33 h, right after the second steering with large angle has begun. This phenomenon is not regarded as natural speed loss, because the engine trouble seems to occur as the result of the emergency operation in the rapid change of sea state. As mentioned, large steering angles are not recommended, especially in the ballast condition. This could induce massive loads on the main engine through the propeller shaft, causing propeller racing, which in turn could trigger the main engine to stop as an emergency action. The main engine resumes 4 min after the suspension, which is a dangerous situation in rough sea voyages. Relative water surfaces at the fore peak and probabilities of slamming are summarized as shown in Figure 25.

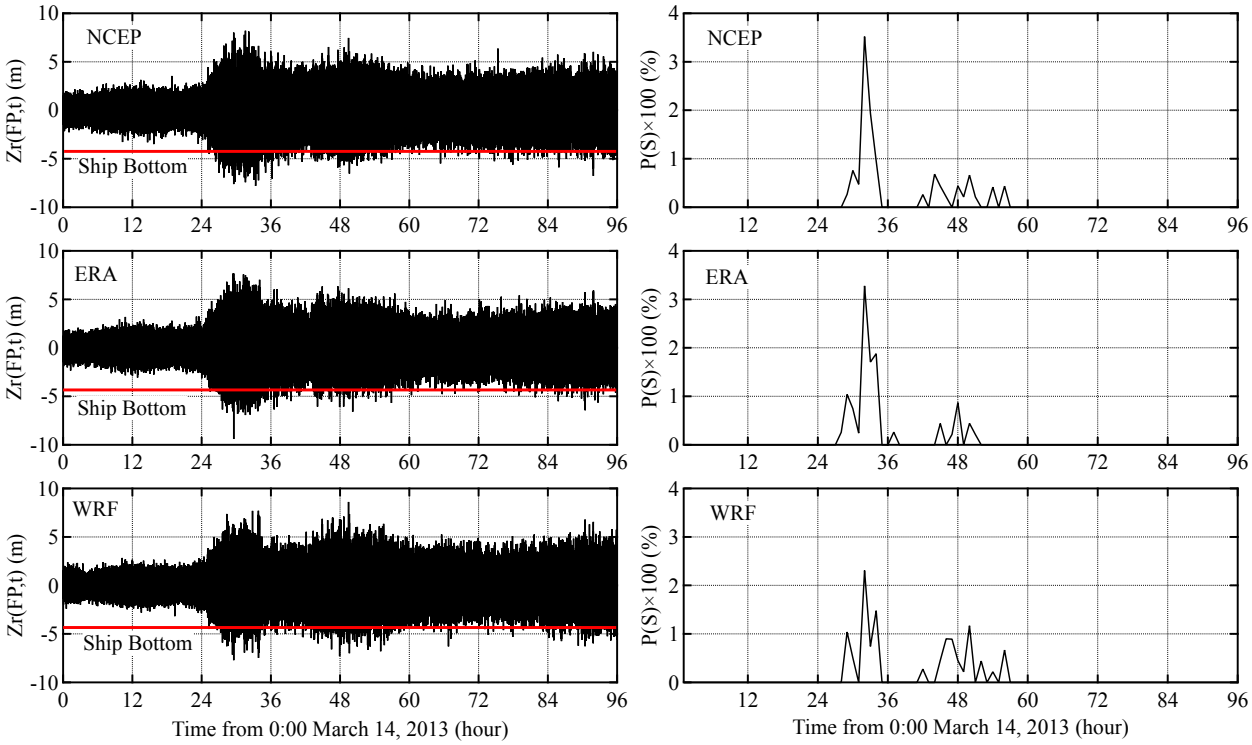

Figure 25 Variations in relative water surfaces and probabilities of slamming (Case C)

Probabilities of slamming are 2.5–3.5% at the maximum, which are close to the probabilities of deck wetness in Case A. As seen in Figure 23, although the maximum value exceeds the criteria in Table 1, deliberate speed reduction occurs at approximately 24 h, which is almost the same time when the possibility of slamming becomes nonzero. Relative water surfaces at the aft peak and the probabilities of propeller racing are summarized in Figure 26.

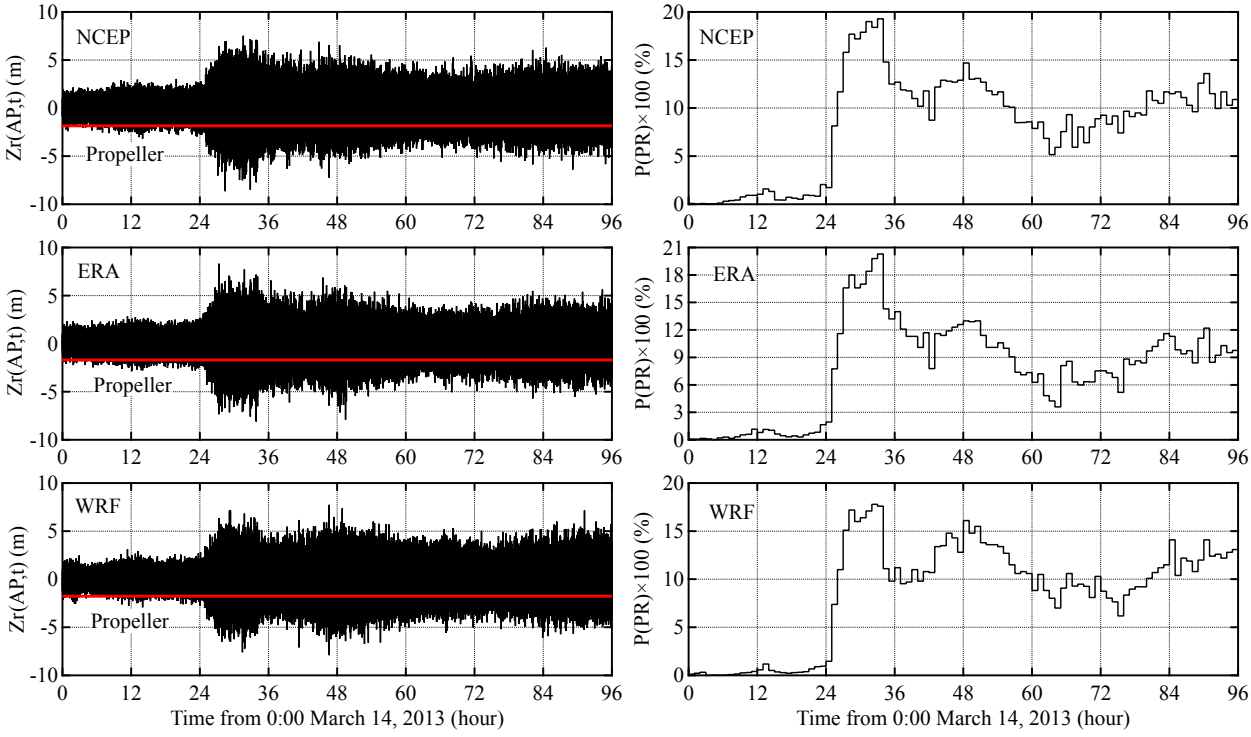

Figure 26 Variations in relative water surfaces and probabilities of propeller racing (Case B)

Probabilities of propeller racing are much higher than those in Cases A and B because of the ballast condition. In Figure 26, propeller racing becomes a nonzero from 24 h and increases remarkably thereafter. The maximum value reaches approximately 20% near 30 h, which is a few hours before the abnormal drop in engine speed. It is shown that the limiting value of vertical acceleration corresponds to the deliberate speed reduction. However, limiting values of lateral acceleration and roll motion do not necessarily agree with the timing of the speed loss. It is also shown that the probabilities of slamming and propeller racing can be used to evaluate the occurrence of deliberate speed reduction at the point where they start to increase from zero.

4.4 Analysis of Engine Parameters in Rough Sea Voyages

The criteria applicable in the ship's bridge, which have been proposed in earlier studies, were validated in the previous section. While in rough sea voyages, the increased resistance to a ship's motion is transmitted to the main engine via the propeller shaft. This sometimes causes engine overload, incomplete combustion, and surging phenomenon in the turbocharger, which are dangerous to ships. Thus, marine engineers monitor various parameters and reduce fuel injection to intentionally lower the engine load. Here, variations in engine parameters are analyzed to identify their relation with speed loss. The analyzed parameters are fuel pump mark (fuel injection per second), engine power, exhaust gas temperature of cylinder, shaft thrust, revolution of blades in the turbocharger, etc.

(1) Case A

Figure 27 shows the variations of fuel pump mark, engine power, exhausted gas temperatures, ship thrust, and revolution of blades in the turbocharger as 1-min average values from June 1–3, 2013.

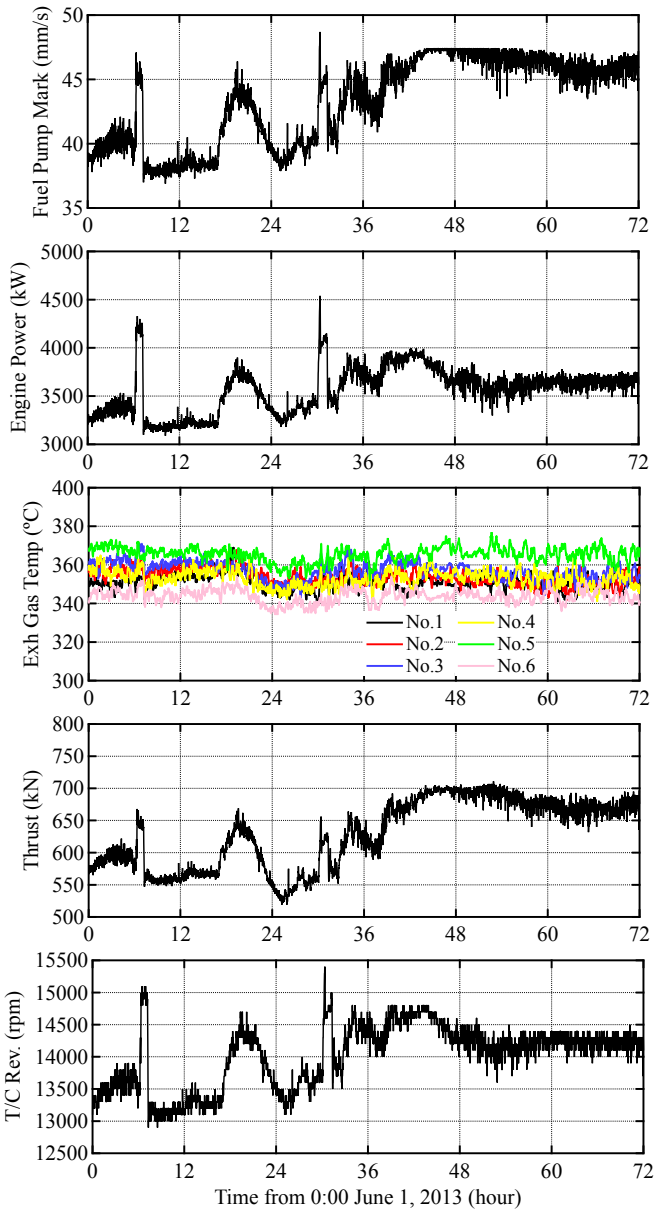

Figure 27 Variations in engine parameters (Case A)

Similar variations can be seen in the fuel pump mark, engine power, shaft thrust, and revolution of blades in the turbocharger in the figure. They increased once at approximately 20 h and reverted to the previous values. Although there are no remarkable fluctuations in vertical acceleration at that time, the gradual speed loss for 2 knots occurs. This operation is thought to prevent speed loss through the added resistance. Engine speed has been almost constant from 20–40 h, except for a temporary rise in automatic multiplication once a day. The engine power becomes a constant after it has slightly decreased at approximately 40 h, when both the ship's speed and engine speed have reduced. In the figure, it is obvious that the temperature of No.5 and No.3 are

higher in all the cylinders. Reasons the exhaust gas temperature is higher include (1) overload, (2) delay in fuel injection, (3) incomplete fuel spray, (4) early opening of exhaust valve, and (6) soot in air pipe (Hasegawa, 2010). Although it is difficult to identify the exact reason in these cases, there is a possibility that any of them can affect the temperature. Decided from the viewpoint of safe engine operation, the risk of incomplete combustion in this case becomes apparent because of the rise in exhaust gas temperature or engine overload when the power is increased more than that in the 40-h case. The alarming increase in added resistance makes it impossible to maintain the ship's speed. The ship's speed is intentionally reduced to avoid the additional increase in exhaust gas temperature, which helps to maintain the safety of the main engine. The decision to cause a deliberate speed reduction can be decided at approximately 40 h, if marine engineers attempt to prevent engine overload and incomplete combustion by monitoring those parameters. The deck wetness and the main engine overload occur at almost the same timing.

(2) Case B

Figure 28 shows the variations in fuel pump mark, engine power, exhausted gas temperatures, ship thrust, and revolutions of the turbo charger as 1-min average values from June 14 to 17, 2013.

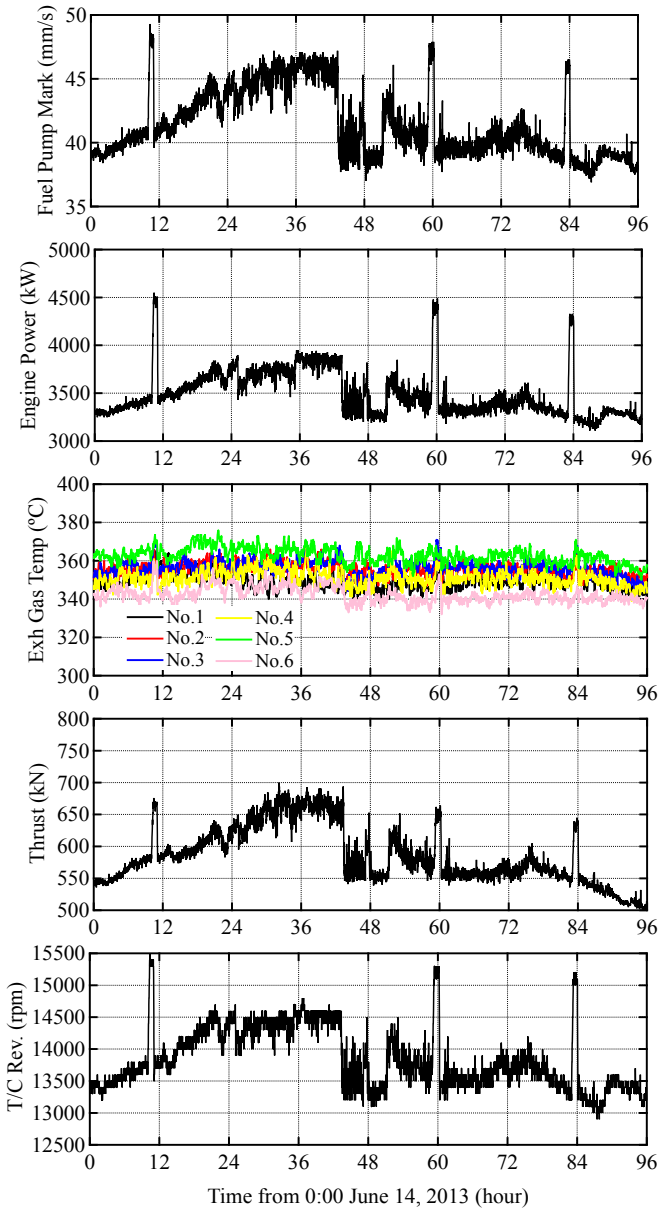

Figure 28 Variations of engine parameters (Case B)

There are similar variations in the fuel pump mark, the engine power, the shaft thrust, and the revolution of blades in the turbocharger, as the same with Case A. Although they once decrease at the same timing with the ship's speed and the engine speed, they have been increasing until 40 h gradually. This pattern is quite different from that in Case A. It implicates that the added resistance is smaller than that in Case A, and the ship can increase engine power here. After 40 h, engine parameters decrease so much because the relative wave direction varies by the steering with large angles. This is a typical pattern of avoiding the overload of main engine by steering with larger angles.

(3) Case C

Figure 29 shows variations of fuel pump mark, the engine power, the exhausted gas temperatures, the ship

thrust, and the revolution of blades in the turbocharger as 1-min average values from March 14 to 17, 2013.

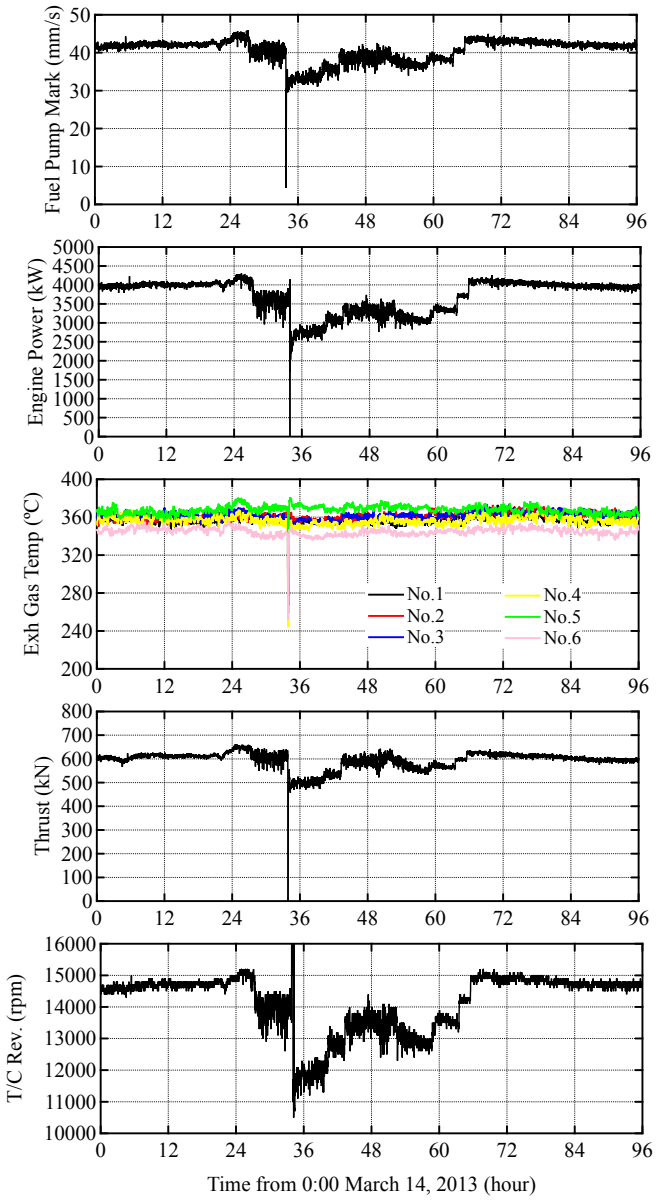

Figure 29 Variations in engine parameters (Case C)

Similar patterns can be seen in fuel pump mark, engine power, shaft thrust, and the revolution of in the turbocharger. These values have been decreased rapidly for 4 min at approximately 30 h. This occurs at the same time as the larger steering angle, and the abnormal situation is caused by steering in rough seas. It is common for a ship to choose the larger steering angles to change the wave direction as in Case B. However, this operation puts the ship in a precarious situation. For this reason, deceleration operations should be conducted in the early stages and avoid large steering angles as much as possible.

(4) Frequency Property of Engine Parameters

As discussed in section 3, the analysis of frequency property of an engine operation is important for rough sea voyages. This is analyzed for the measured data via a fast Fourier transformation (FFT) algorithm. According to the questionnaire, time periods of the emergency operation range from several minutes to an hour or so. Data length is set as 6 h with the sampling time at 1 s for the FFT analysis. The spectra of engine speed, fuel pump mark, revolution of blades in the turbocharger, and ship speed are shown for the calm sea state in May 12, 2013 and the rough sea state in June 3, 2013 in Figures 30–31.

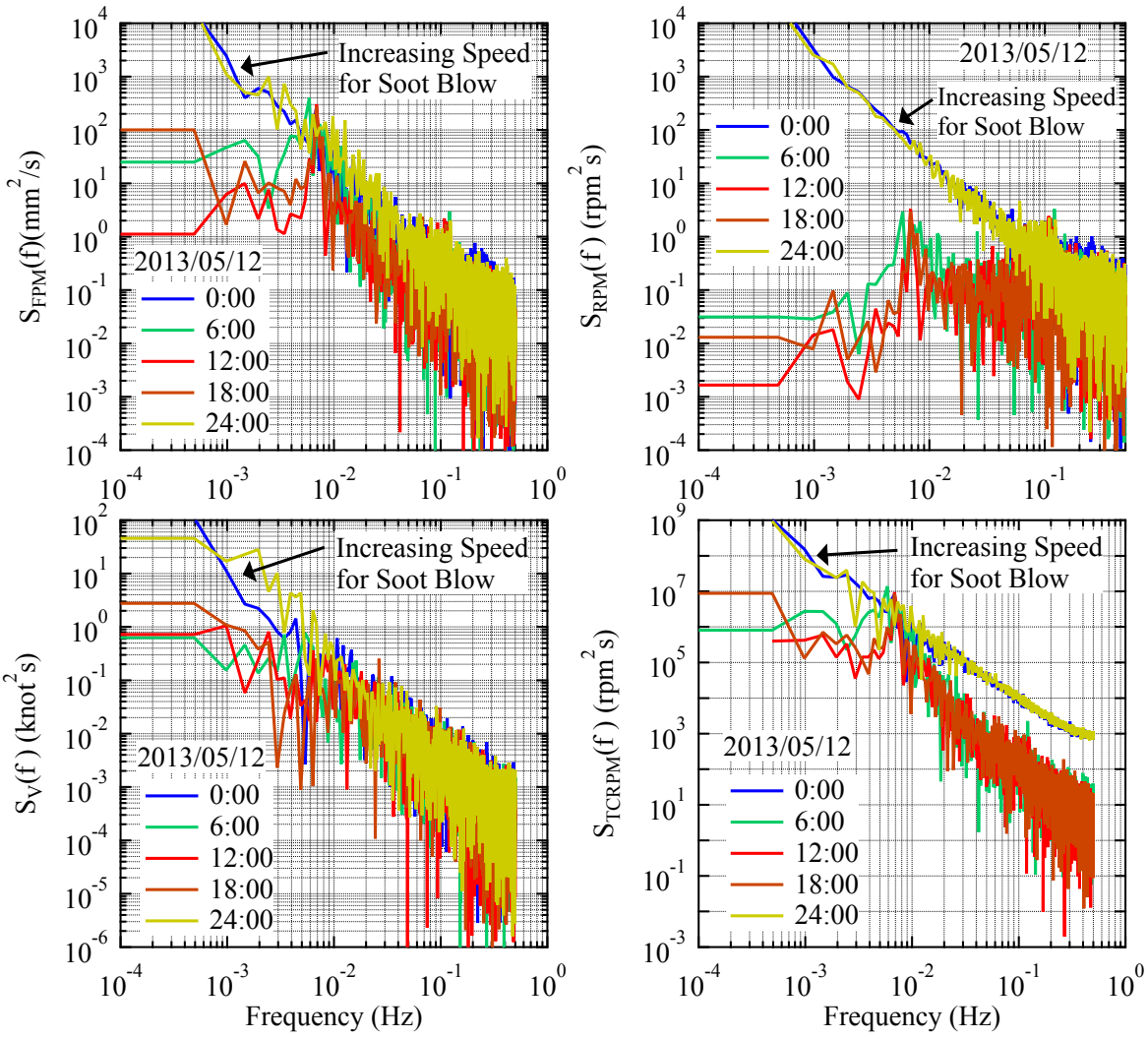

Figure 30 Spectra of engine parameters in calm sea state (May 12, 2013)

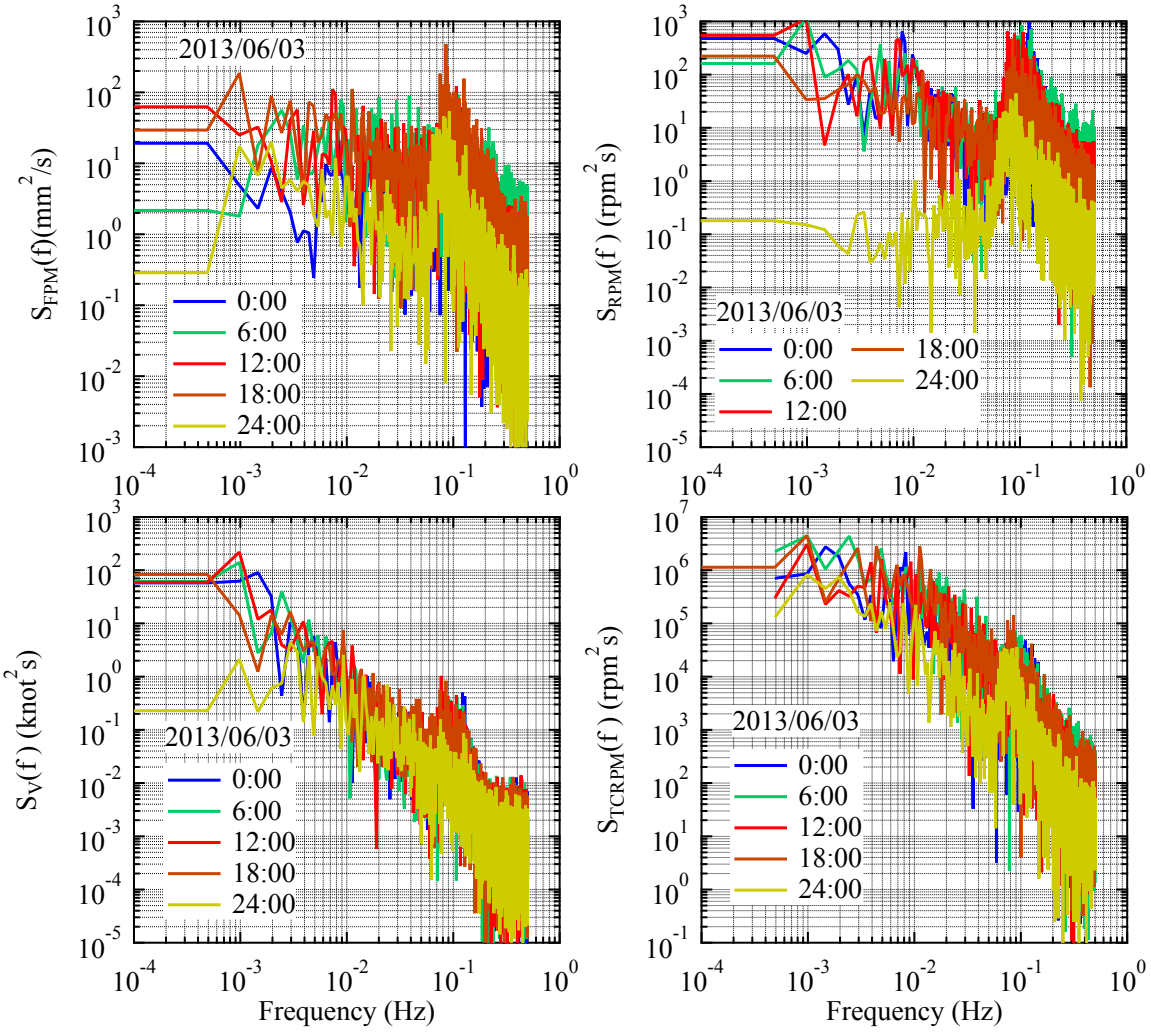

Figure 31 Spectra of engine parameters in rough sea state (June 3, 2013)

In Figure 30, peaks can be observed from 0.005 to 0.008 Hz (125–200 s) for the spectrum of engine speed in the calm sea state. Similar peaks can be seen in the spectrum in the rough sea state on the right-hand side, too. This frequency range corresponds to the autopilot steering frequency. There are two different spectrum shapes in the figures on the left representing the instant when the ship automatically accelerates from 12 to 14 knots. The ship then decelerates from 14 knots (the navigation full speed) to conserve fuel, and it is necessary to increase the speed for the soot blow at the funnel once a day. In Figure 31, strong peaks appear around 0.1 Hz (10 s) in all types of spectra. It is obvious that they are components influenced by ship motions on the waves. Furthermore, strong peaks appear from 0.001–0.002 Hz (500–1,000 s). It is shown that the main period of emergency engine operations ranges from 10 min to 1 h. Peak frequencies measured from 0.001 to 0.002 Hz are similar to those of the period of emergency engine operations. This indicates that the results of the questionnaire can be validated with the analyzed results of measured data. It is shown that three types of periods exist in the variations of engine parameters:

(A) approximately 10–15 s due to ship motions on waves

(B) 125–200 s due to autopilot or manual steering

(C) 500–1,000 s due to emergency operations to decelerate

It is shown that components of (A) and (C) add to (B) in rough sea voyages, and these parameters can be estimated as the summation of the frequency components corresponding to these three types of time periods.

5. Results and Discussion

The probabilities of deck wetness, slamming, and propeller racing can be effective measures to evaluate deliberate speed reduction. In previous studies, speed loss occurs before the probabilities reach their limiting values of 2.5% or 5%. However, speed loss occurs right after the probabilities have exceeded zero, and its range depends on the values of these probabilities. The difference with the current seafarers might influence the analyzed results of deliberate speed reduction. First, correlations between the pitch motion and probabilities of deck wetness and propeller racing are analyzed. Estimation formulas are established and validated against measured data. Second, relations between the speed loss and probabilities are analyzed. The speed loss properties are considered with the analyzed results. Correlations are obtained from the measured results of Cases A and B, but Case C is excluded from the calculation due to the difference of loaded conditions and few number of data. These results are only validated for the 28,000-DWT-class bulk carrier. The applicability for other types of ships should be considered using a measurement database in future studies. It is obvious that the probabilities of deck wetness and propeller racing should be estimated from the pitch motion. Thus, the following formula is modeled as a simple quadratic curve.

$$\text{Prob} = \begin{cases} 0 & (0 \le X_{PS} \le b) \\ a(X_{PS} - b)^2 & (b \le X_{PS}) \end{cases}, \tag{18}$$

where, *Prob* is the probability of deck wetness or propeller racing and X_{PS} is the pitch motion. It is characteristic of the probabilities to be zero from the origin to a certain value in the *x*-axis, and the value rapidly increases as nonlinear functions. In Eq. (18), the boundary point, b, is defined as 2.5° for the pitch motion. The value of b is decided when the determinant coefficient is the highest (the most fitting with measured data) in several values. The relations between probabilities of deck wetness, propeller racing, and pitch motion are shown in Figures 32–33.

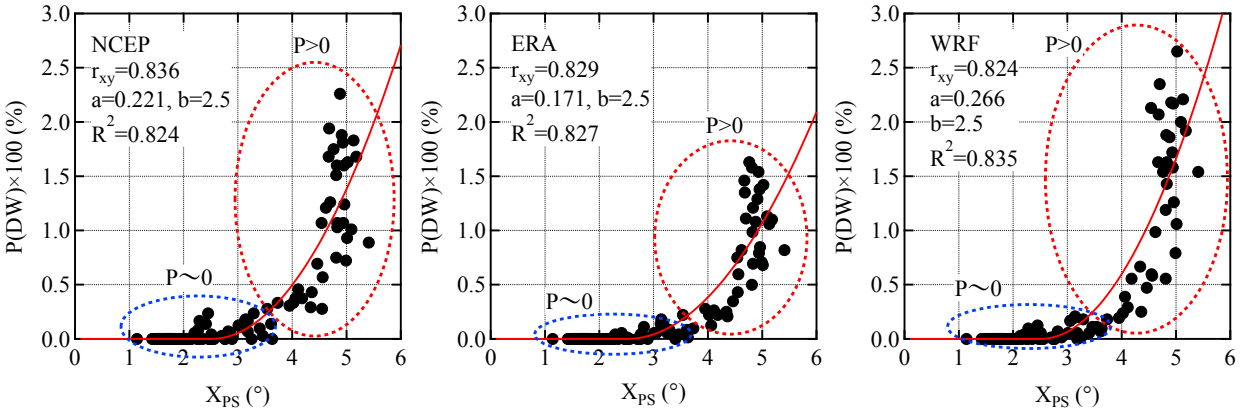

Figure 32 Relations and fitting curves between pitch motion and probability of deck wetness

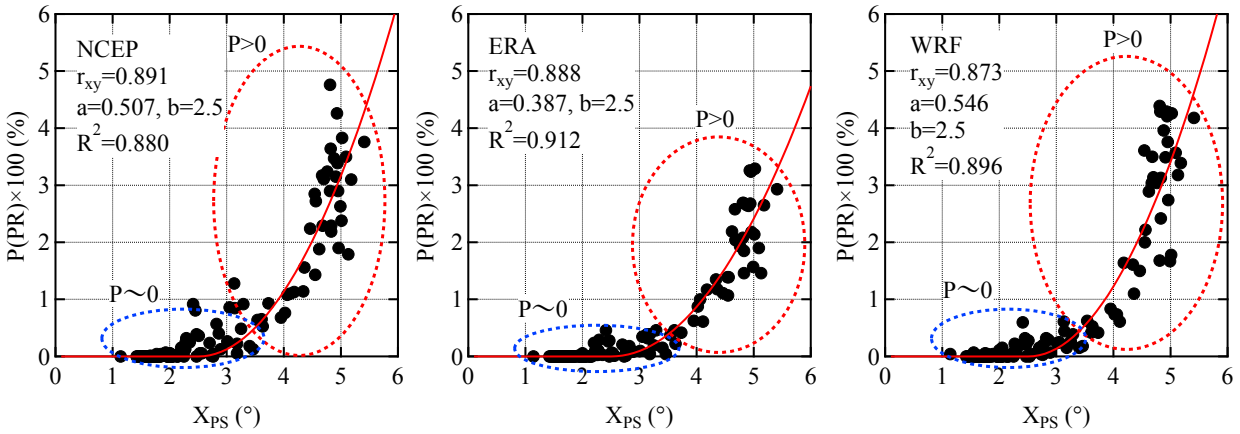

Figure 33 Relations and fitted curves between pitch motion and probability of propeller racing

The probability of deck wetness has high correlations of 0.836, 0.829, and 0.824 with the pitch motion. There are also higher correlations with respect to the probability of propeller racing, 0.891, 0.888, and 0.873, that is, approximately 0.9. Probabilities are almost zero when the pitch motion is less than 2.5–3.0°, where deliberate speed reduction has not occurred yet. These values rapidly increase from the boundary point and can be well fitted by the quadratic curves. The coefficients of determination are 0.824, 0.827, and 0.835 for the deck wetness and 0.880, 0.912, and 0.896 for propeller racing. This means that the probability of deck wetness and propeller racing tend to be proportionate with the square of pitch motion, in a region above the boundary point of 2.5–3.0°. Relations between the speed loss and these probabilities are shown in Figures 34–35.

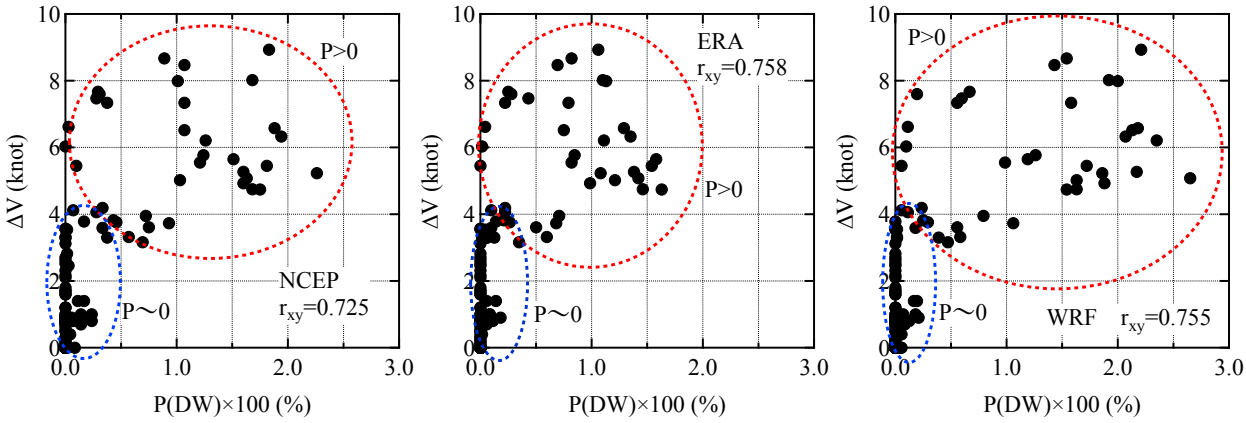

Figure 34 Relations between the speed loss and probability of deck wetness

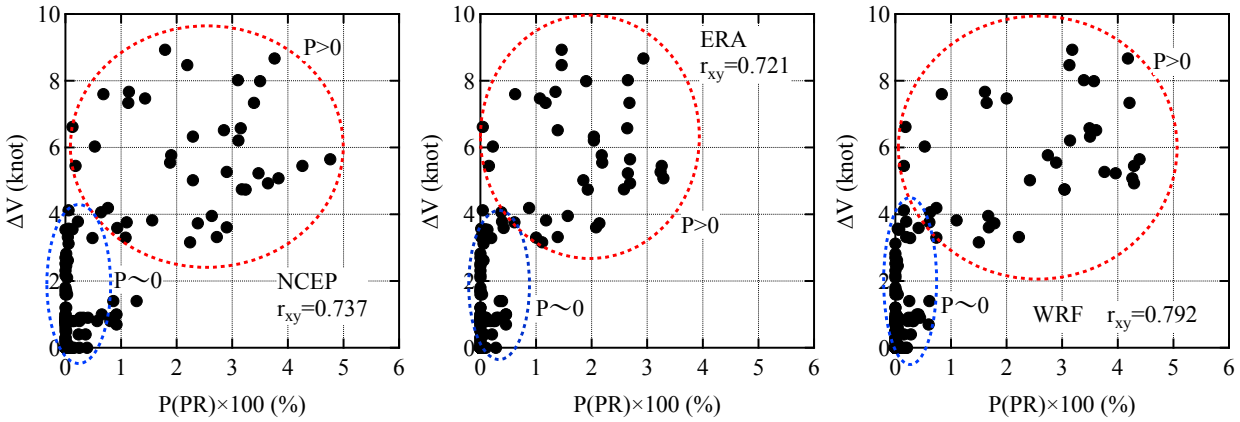

Figure 35 Relations between the speed loss and probability of propeller racing

In these figures, the speed loss, ΔV, is defined as $\Delta V = 12.0 - V$. It is obvious that the values of $P(DW)$ and $P(PR)$ are almost zero when $\Delta V < 3$–4 knots, which is the boundary area. They significantly increase in the region above the boundary area, which is indicated by a dotted red circle. However, the plotted points appear to have large variability, although the correlation coefficients are not very low, that is, they are 0.7–0.8. It seems necessary to accumulate more measured data in various sea and loading conditions. to estimate the speed loss from probabilities of deck wetness or propeller racing. Relations between the speed loss and the main wave direction are shown in Figure 36. The wave direction is defined as 0° for the head sea state and 180° for the following sea state.

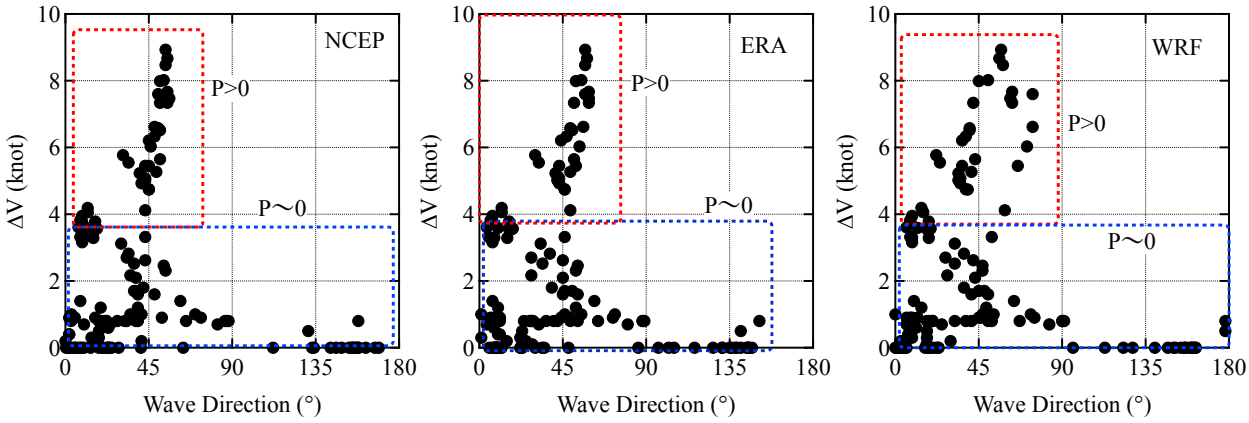

Figure 36 Relation between the speed loss and the main wave direction

Speed loss greater than 4 knots is primarily observed at approximately 45–60°. These speed losses are not commonly observed in the head sea state. This implies that the ship empirically avoids the head sea or beam sea states. This is the same as the rough sea maneuvering shown in section 2. In this situation, the longitudinal motions were dominant with the speed loss, which was not observed in the range of 90–180°, as described in the seakeeping theory (Kashiwagi, et al., 2004). The relation between the speed loss and the pitch motion is analyzed as shown in Figure 37.

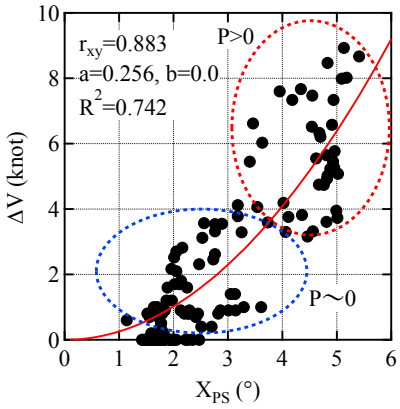

Figure 37 Relation between the speed loss and the pitch motion

The correlation coefficient is 0.883, and the speed loss, ΔV, is fitted by Eq. (15). The coefficient of determination is 0.742, which is lower for 0.1 than for probabilities of deck wetness and propeller racing. This uncertainty might be related on the complexity of deliberate speed reduction. Currently, the analyzed results are still limited. Further analysis will be conducted to accurately evaluate the speed loss.

6. Conclusions

This study analyzes and evaluates speed loss during rough sea voyages and reproduces the validity of previous studies for a 28,000-DWT-class bulk carrier in rough sea conditions. The limiting value of vertical acceleration shows nearly the same timing as the measured result. On the other hand, the limiting values of lateral acceleration or roll motion are smaller than the measured result. Although the limiting values of the probabilities of deck wetness or slamming are defined as 2.5 or 5%, deliberate speed reduction occurs at the point when the probability exceeds zero, initial stage of deck wetness, slamming, or propeller racing. Detailed variations of engine parameters are summarized in rough sea voyages, and they have very similar, time-varying properties. There are two patterns of engine operations at the point where natural speed loss switches on to the deliberate speed reduction. One is making fuel injection rate constant after increasing it to maintain engine speed, as shown in Case A. The second one is making fuel injection rate constant after it has decreased once due to the large steering angle, as shown in Case B. It is also shown (Case C) that steering sometimes causes temporary engine failure in turbulent sea conditions. The frequency property of engine operations was analyzed, and additional peaks around 10 s and 500–1,000 s were observed due to ship motions and intentional handling of machines in rough sea voyages besides the frequency of autopilot being approximately 125–200 s. These time periods of operations could affect the deliberate speed reduction, and agree with the results of the questionnaire. The correlation coefficients are high (0.82–0.89) between the pitch motion and the probabilities of deck wetness or propeller racing. The simple estimations are modeled as the quadratic curves, which have a high coefficient of determination (0.82–0.91). It confirms that the probabilities of deck wetness or propeller racing can be expressed as a quadratic function of pitch motion. When the amount of speed loss is discussed, the probability of deck wetness or propeller racing is almost zero in $\Delta V <$ 3–4 knots. This implies that deliberate speed reduction may occur when the speed loss exceeds 3–4 knots. There are some dispersions between the speed loss and the probabilities for $\Delta V >$ 3–4 knots. The speed loss for $\Delta V >$ 3–4 knots occurs when the main wave direction is approximately 45° from the bow. Considering the influence of the longitudinal motions, they have a relatively good correlation with measured the speed loss. However, the coefficient of determination decreases to 0.742. This may be caused by the uncertainty of speed loss, including the deliberate speed reduction. The criteria for bulk carrier is mainly summarized as the 0.15g of vertical acceleration at ship's bridge, which is the same as the former study. On the other hand, the probability of deck wetness and propeller racing should be revised as 0–0.5%, which corresponds with 3° of pitch motion. It is also shown that the roll motion or lateral acceleration does not lead to the deliberate speed reduction very much. A further analysis of the measured data must be conducted for different sea regions, weather conditions, loading conditions, ship types, etc. Based on this study, the estimation of speed loss will be more accurate for the practical use in the optimal ship routing.

Acknowledgements

The authors wish to extend their gratitude to Shoei Kisen Kaisha, Ltd., for their cooperation in conducting onboard measurements of the 28,000-DWT bulk carrier from 2010 to 2016. In addition, we would like to thank Mr. Yoshikazu Tanaka and Mr. Hiroyuki Oda, MOL Techno-Trade, Ltd., Japan, and Dr. Takashi Miwa, Kobe University, Japan, for their guidance in rough sea voyage and marine engine operations. This study was financially supported by Scientific Research (B) (Project No. 16H03135, 2016-2018, represented by Kenji Sasa), Challenging Explanatory Research (Project No. 15K12474, 2015-2017, represented by Kenji Sasa), and Fostering Joint International Research (B) (Project No. 18KK0131, 2018-2022, represented by Kenji Sasa) under Grants-in-Aid for Scientific Research, Japan Society for Promotion and Science. This study was also supported by the Croatian Science Foundation under project IP-2018-01-3739 (represented by Jasna Prpić-Oršić).

References

Aertssen, G., 1967. Labouring of ships in rough seas with special emphasis on the fast ship, In: Society of Naval Architects and Marine Engineers (SNAME) diamond Jubilee International Meeting, pp.1-34.

Aertssen, G. and Van Sluys, M.F., 1972. Service performance and seakeeping trials on a large containership, In: Transactions of Royal Institution of Naval Architects (RINA), Vol.114, pp.429-447.

Dee, D.P., et al., 2011. The ERA-interim reanalysis, configuration and performance of the data assimilation system, Q. J. R. Meteorology Society, Vol.137, No.656, pp.553-597.

DNV-GL, 2016. Technology outlook 2025, 85p.

Faltinsen, O.M., 1993. Sea loads on ships and offshore structures, Cambridge University Press, 328p.

Faltinsen, O.M., Minsaas, K.J., Liapis, N. and Skjørdal, S., 1980. Prediction of resistance and propulsion of a ship in a seaway, In: Proceedings of the 13th Symposium on Naval Hydrodynamics, pp. 505-529.

Gerritsma, J., 1984. Practical use of ship motion calculations for design and operation of ships, Technische Hogeschool Delft, Lab. Voor Scheepshydromechanica, pp.1-24.

Hagiwara, H., Shoji, R., and Sugisaki, A., 1997, A new method of ship weather routing using neural network, Journal of the Tokyo University of Mercantile Marine, Natural Sciences, Vol.47, pp.21-29.

Hanssen, G.L., and James, R.W., 1960. Optimum ship routing, J. Institute of Navigation, Vol.13, No.3, pp.253-272.

Hasegawa, S., 2010. Instruction of marine diesel engine, Seizando Shoten, 410p. (in Japanese)

Honda, K., 1980. Ship handling theory, Seizando Shoten, pp.179-200, (in Japanese).

Kalnay, E., et al., 1996. The NCEP/NCAR 40-year reanalysis project, Bulletin of American Meteorology Society, Vol.77, No.3, pp.437-471.

Kashiwagi, M., 1991. Calculation formulas for the wave-induced steady horizontal force and yaw moment on a ship with forward speed, Report of Research Institute of Applied Mechanics of Kyushu Univ., Vol.37, No.107, pp.1-18.

Kashiwagi, M., 1992. Added resistance, wave-induced steady sway force and yaw moment on an advancing ship, Ship Technology Research, Vol.39, pp.3-16.

Kashiwagi, M., Sugimoto, K., Ueda, T., Yamasaki, K., Arihama, K., Kimura, K., Yamashita, R., Ito, A., Mizokami, S., 2004. An analysis system for propulsive performance in waves, J. Kansai Society of Naval Architects of Japan Vol.241, pp.1–16, (in Japanese).

Kim, S.K., Naito, S., and Nakamura, S., 1984. The evaluation of seakeeping performance of a ship in waves, J. Society of Naval Architects of Japan, Vol.155, pp.71-83, (in Japanese).

Kitazawa, T., Kuroi, M., and Takagi, M., 1975. Critical speed of a container ship in rough sea, J. Society of Naval Architects of Japan, Vol.138, pp.269-276, (in Japanese).

Lin, Y.H., Fang, M.C. and Yeung, R.W., 2013. The optimization of ship weather routing algorithm based on the composite inuence of multi-dynamic elements, J. Applied Ocean Research, Vol.43, pp.184-194.

Lu, L.F., Sasa, K., Sasaki, W., Terada, D., Kano, T., and Mizojiri, T., 2017. Rough wave simulation and validation using onboard ship motion data in the Southern Hemisphere to enhance ship weather routing, J. Ocean Engineering, Vol.144, pp.61-77.

Maki, A., Akimoto, Y., Nagata, Y., Kobayashi, S., Kobayashi, E., Shiotani, S., Ohsawa, T., and Umeda, N., 2011. A new weather-routing system that accounts for ship stability based on a real-coded genetic algorithm, J. Marine Science and Technology, Vol.16, pp.311-322.

Ministry of Land, Infrastructure, Transport and Tourism, 2013. White paper on land, infrastructure, transport and tourism in Japan, 2012, http://www.mlit.go.jp/english/white-paper/2012.pdf, pp.154-215.

Naito, S., Nakamura, S., and Hara, S., 1979. On the prediction of speed loss of a ship in waves, J. Society of Naval Architects of Japan, Vol.146, pp.147-156, (in Japanese).

NordForsk, 1987. Assessment of ship performance in a seaway, 91p.

Ochi, M.K. and Motter, L.E., 1974. Prediction of extreme ship responses in rough seas of the North Atlantic, In: Proceedings of the International Symposium on Dynamics of Marine Vehicles and Structures in Waves, pp 187-197.

Okusu, M., 1986. Added resistance of blunt bow ships in very short waves, J. Kansai Society of Naval Architects of Japan, Vol.202, pp.39-42.

Prpić-Oršić, J. and Faltinsen, O.M., 2012. Estimation of speed loss and associated CO_2 emissions in a seaway, J. Ocean Engineering, Vol.44, pp.1-10.

Qinetiq, Lloyd's Register, and Univ. of Strathclyde, 2013. Global marine trends 2030, 144p.

Sasa, K., Terada, D., Shiotani, S., Wakabayashi, N., Ikebuchi, T., Chen, C., Takayama, A., and Uchida, M., 2015. Evaluation of ship performance in international maritime transportation using an onboard observation system—in case of a bulk carrier for international voyages—, J. Ocean Engineering, Vol.104, pp.294-309.

Sasa, K., Faltinsen, O.M., Lu, L.F., Sasaki, W., Prpić-Oršić, J., Kashiwagi, M., and Ikebuchi, T., 2017. Development and validation of speed loss for a blunt-shaped ship in two rough sea voyages in the Southern

Hemisphere, J. Ocean Engineering, Vol.142, pp.577-596.

Shamarock, W.C., Klemp, J.B., Dudhia, J., Gill, D.O., Barker, D.M., Duda, M.G., Huang, X.Y., Wang, W., Powers, J.G., 2008. A description of the advanced research WRF version 3, NCAR Technical Note NCAR/TN-475+STR, 113p.

Smogeli, O.N., 2006. Control of marine propellers from normal to extreme conditions, Ph.D Thesis of Dept. of Marine Engineering and Science, NTNU, 242p.

Tolman, H.L., 2002. Validation of WaveWATCH III version 1.15 for a global domain, NOAA/NWS/NCEP/OMB Technical Note, No.213, 33p.